

+ B 09 f 3 a
AEDC-TR-66-121 ✓



**IDEAL GAS SPHERICALLY BLUNTED CONE
FLOW FIELD SOLUTIONS
AT HYPERSONIC CONDITIONS**

**J. F. Roberts, Clark H. Lewis, and Marvin Reed
ARO, Inc.**

August 1966

Distribution of this document is unlimited.

**VON KÁRMÁN GAS DYNAMICS FACILITY
ARNOLD ENGINEERING DEVELOPMENT CENTER
AIR FORCE SYSTEMS COMMAND
ARNOLD AIR FORCE STATION, TENNESSEE**

DES
JF
my
time
RJ
aws

NOTICES

When U. S. Government drawings specifications, or other data are used for any purpose other than a definitely related Government procurement operation, the Government thereby incurs no responsibility nor any obligation whatsoever, and the fact that the Government may have formulated, furnished, or in any way supplied the said drawings, specifications, or other data, is not to be regarded by implication or otherwise, or in any manner licensing the holder or any other person or corporation, or conveying any rights or permission to manufacture, use, or sell any patented invention that may in any way be related thereto.

Qualified users may obtain copies of this report from the Defense Documentation Center.

References to named commercial products in this report are not to be considered in any sense as an endorsement of the product by the United States Air Force or the Government.

IDEAL GAS SPHERICALLY BLUNTED CONE
FLOW FIELD SOLUTIONS
AT HYPERSONIC CONDITIONS

J. F. Roberts, Clark H. Lewis, and Marvin Reed
ARO, Inc.

Distribution of this document is unlimited.

FOREWORD

The work reported herein was done at the request of Headquarters, Arnold Engineering Development Center (AEDC), Air Force Systems Command (AFSC), under Program Element 62405334, Project 8953, Task 895303.

The results presented were obtained by ARO, Inc. (a subsidiary of Sverdrup & Parcel and Associates, Inc.), contract operator of the AEDC, AFSC, Arnold Air Force Station, Tennessee, under Contract AF40(600)-1200. The research was conducted under ARO Project No. VW3507, and the manuscript was submitted for publication on May 26, 1966.

The authors are pleased to acknowledge the assistance of W. C. Moger, Central Computer Operations, ARO, Inc., in making the inviscid sharp cone machine calculations. The plots were prepared by M. Brown, Jr. and Thelbert Shields, ARO, Inc., of the von Kármán Gas Dynamics Facility, AEDC.

This technical report has been reviewed and is approved.

Larry R. Walter
Captain, USAF
Research Division
Directorate of Plans and Technology

Donald D. Carlson
Colonel, USAF
Director of Plans and Technology

ABSTRACT

Charts of surface pressures, Mach number, and Reynolds number distributions over spherically blunted cones in an ideal gas ($\gamma = 1.4$) are presented in the ranges $M_\infty = 8$ to 30 and cone half-angles $\theta_c = 0$ to 20 deg. The pressure data are correlated with $C_p/2\theta_c^2$ against $X_c = (x/d_n) \left[\theta_c^2 / (\epsilon k)^{1/2} \right]$ and compared with a previous empirical correlation of experimental data. The difference in numerical results and empirical correlation of surface pressures is attributed to the viscous-induced pressure increment in the experimental data.

CONTENTS

	<u>Page</u>
ABSTRACT.	iii
NOMENCLATURE.	v
I. INTRODUCTION	1
II. CALCULATION PROCEDURE	1
III. RESULTS AND DISCUSSION	2
IV. CONCLUDING REMARKS	4
REFERENCES	4

ILLUSTRATIONS

Figure

1. Surface Pressure Distributions	7
2. Comparison of Inviscid, Ideal Gas ($\gamma = 1.4$) Surface Pressure Distributions	22
3. Pressure Distribution on a Sphere: Comparison of Approximate Theories with the Present Numerical Results	23
4. Surface Mach Number Distributions over Sharp and Blunt Cones	24
5. Surface-to-Free-Stream Reynolds Number Ratio for Sharp and Blunt Cones	32
6. Correlation of Surface Pressure Distributions for Blunt Cones	40

NOMENCLATURE

C_p	Pressure coefficient, $2(p - p_\infty) / p_\infty \gamma M_\infty^2$
d_n	Nose (sphere) diameter
k	Nose drag coefficient
M	Mach number
p	Pressure
R_o	Nose (sphere) radius

Re	Reynolds number
S/R_o	Dimensionless surface distance measured from forward stagnation point
X_c	Cheng's axial correlation parameter, $(x/d_n) \left[\theta_c^2 / (\epsilon k)^{1/2} \right]$
x	Axial distance from forward stagnation point
γ	Ratio of specific heats
ϵ	Normal shock density ratio, $(\gamma - 1) / (\gamma + 1)$
θ_c	Cone half-angle

SUBSCRIPTS

o'	Normal shock (pitot) stagnation conditions
w	At the (inviscid) wall or surface
∞	Free-stream conditions

SECTION I INTRODUCTION

For various aerodynamic investigations, inviscid solutions for spherically blunted cones are needed. The lack of extensive exact solutions encouraged the authors to compute ideal gas ($\gamma = 1.4$) flow fields over spherically blunted cones for a Mach number range from 8 to 30 and a range of cone half-angles, θ_c , from 0 to 20 deg.

The Russian data of Chushkin and Shulishnina (Ref. 1) in the Mach number range, M_∞ , from 3 to 10 and infinity for $\theta_c = 0, 3, 5, 10, 20, 30$, and 40 deg were presented in tabular and graphical form by Ellett (Ref. 2). Unfortunately, the scales of some of the plots in Ref. 2 are such that reading the values accurately is difficult. Moreover, only the pressure coefficient, C_p , and wall-to-stagnation pressure ratio, p_w/p_o' , were presented.

The present report gives p_w/p_o' , M_w , and Re/Re_∞ as functions of surface distance, S/R_o , for spherically blunted cones. In addition, the parameter $C_p/2\theta_c^2$ against $X_c \equiv (x/d_n)[\theta_c^2/(ek)]^{1/2}$ is also presented. The parameter $C_p/2\theta_c^2$ was proposed by Griffith and Lewis (Ref. 3) who modified Cheng's (Ref. 4) correlation parameter $p_w/p_\infty M_\infty^2 \gamma_\infty \theta_c^2$ in order to obtain better correlation of experimental data over a range of Mach and Reynolds numbers (see Ref. 3). The correlation variable X_c was proposed by Cheng and was found to correlate the experimental data well. A comparison of the correlated ideal gas calculations with the empirical correlation of experimental data by Griffith and Lewis is also presented herein.

SECTION II CALCULATION PROCEDURE

The spherically blunted cone solutions were obtained with an IBM 7094 program similar to the one developed by Lomax and Inouye (Ref. 5) and Inouye, Rakich, and Lomax (Ref. 6) at NASA Ames Research Center. A method similar to the Ames procedure noted above was recently developed by Christensen (Ref. 7) and includes attached and laminar separated boundary layers in addition to ideal and equilibrium gas inviscid outer flow.

All of the ideal gas flow field results in the present report were obtained for spherically blunted cones at sea-level conditions. Since the

flow field calculations considered only an ideal gas, the choice of free-stream conditions is arbitrary. The Reynolds number is affected, however, through the choice of viscosity law and (free-stream) reference conditions.

The machine program for the blunt body solution was chained to the program for the characteristics solution such that only the free-stream conditions, sphere-cone geometry, and a few initial guesses were specified (see, e.g., Refs. 6 and 7). For the results reported herein, the surface pressure distribution along the body was of primary importance. Machine cards were punched from these data, and a separate program was written to compute p_w/p_o , M_w , Re/Re_∞ , and $C_p/2\theta_c^2$. The calculations were terminated when the surface pressure had reached the inviscid sharp cone value. Although the blunt and sharp cone surface pressures approached the same limit far downstream from the nose or apex, the blunt cone surface temperature, density, and velocity, of course, were affected by the normal shock stagnation pressure loss.

For convenience and comparison with the blunt cone results, the surface conditions for sharp cones of the same cone half-angle and free-stream conditions were computed and are presented herein. The procedure used was similar to that described by Sims (Ref. 8), and comparisons with his results showed good agreement.

SECTION III RESULTS AND DISCUSSION

The inviscid, ideal gas ($\gamma = 1.4$) surface pressure distributions over spherically blunted cones in the ranges $\theta_c = 0$ to 20 deg and $M_\infty = 8$ to 30 are shown in Fig. 1. For convenience the data are shown for fixed cone half-angle and variable M_∞ and vice versa. The sharp cone asymptotic limits are also shown. As noted earlier, the blunt cone solutions were terminated when the surface pressure had clearly reached the asymptotic limit. For small θ_c and large M_∞ , this required perhaps a few hundred nose radii. The results shown in Fig. 1 were only plotted to $S/R_o = 150$ to permit the largest practical scale for reading and graphical interpolation.

A comparison with the data of Chushkin and Shulishnina at $M_\infty = 10$ as given by Ellett (Ref. 2) is shown in Fig. 2. The agreement is good except for the last point on the hemisphere-cylinder. Since no other data were given in Ref. 2 between $S/R_o = 36.17$ and 68.17, the cause for this disagreement is unknown. In general, however, it can be seen that the agreement is good, and the present results can be considered as an extension of those of Chushkin and Shulishnina (Ref. 1).

It is well known that the approximate Newtonian and Newtonian/Prandtl-Meyer theories are useful in predicting the pressure distribution over spheres at high Mach numbers. Figure 3 shows a comparison of these approximate theories with the present blunt body solutions at $M_\infty = 8$ and 30. The fact that the inviscid blunt body solutions lie below the approximate theories by as much as 10 percent can be significant when comparing experimental data with the approximate theories. That is, good agreement between experimental data and the approximate theories does not necessarily imply the absence of viscous effects on the blunt body pressure distribution. The point is made here to caution potential users of these data against expecting too great an accuracy from the use of inviscid solutions and approximate theories.

The surface Mach number distributions are shown in Fig. 4. The inviscid sharp cone solutions are shown in Fig. 4a for convenience. The data given in Fig. 4 might be useful, for example, in estimating conditions at the "edge" of the boundary layer in boundary-layer separation and transition studies. As with the other data presented, the plots were made such that graphical interpolations of the data could be made. Also as in the plots of surface pressure distributions, the effects of M_∞ and θ_c on the nose-dominated region is clearly evident from Fig. 4.

A plot of surface-to-free-stream Reynolds number ratio, Re/Re_∞ , is given in Fig. 5 where Sutherland's viscosity law was used. The sharp cone results are shown in Fig. 5a, and the blunt cone results at discrete M_∞ are given in Figs. 5b to h. As for the surface Mach number, these results might be useful in some perfect gas boundary-layer studies.

The correlation parameter $C_p/2\theta_c^2$ against $X_c = (x/d_n) \left[\theta_c^2 / (\epsilon k)^{1/2} \right]$ is shown in Fig. 6. The present numerical results are compared with the previous empirical correlation results of Griffith and Lewis (Ref. 3). Presentation in this way clearly shows the large difference between the inviscid surface pressure and the correlation of experimental data over a rather wide range of conditions (see Ref. 3). Excluding the $M_\infty = 8$ and $\theta_c = 20$ -deg curve, the minimum pressure for the remaining data shown was correlated within a bandwidth of 13 percent. If θ_c^2 is replaced by $\sin^2 \theta_c$, the bandwidth is increased to about 20 percent. The results shown here thus add to the validity of the correlation parameter used by Griffith and Lewis and clearly show a substantial difference which is attributed to a viscous-induced pressure increment in the previous empirical data. An uncertainty remains as to the "real gas effects" on the experimentally measured surface pressures; however, this effect is believed small for the range of experimental data considered in Ref. 3.

SECTION IV CONCLUDING REMARKS

Ideal gas ($\gamma = 1.4$) surface pressure, Mach number, and Reynolds number distributions for spherically blunted cones have been computed in the ranges $M_\infty = 8$ to 30 and $\theta_c = 0$ to 20 deg. Comparisons with earlier calculations over a more limited range of conditions indicated good agreement. Comparisons with approximate theories indicated differences in surface pressures over a sphere as large as 10 percent. Also comparisons with empirical correlations of experimental surface pressure distributions clearly indicated a difference which was attributed to the viscous-induced pressure increment. Finally, the present numerical results are plotted to scales that would permit graphical interpolations of the data to be made.

REFERENCES

1. Chushkin, P. I. and Shulishnina, N. P. Tables of Supersonic Flow about Blunted Cones, Academy of Sciences, USSR Computation Computation Center Monograph, 1961. Translated and Edited by J. F. Springfield, AVCO Tech. Memo RAD-TM-62-63, September 1962.
2. Ellett, D. M. "Pressure Distributions on Sphere Cones." Sandia Corporation Research Report SC-RR-64-1796, January 1965.
3. Griffith, B. J. and Lewis, C. H. "A Study of Laminar Heat Transfer to Spherically Blunted Cones and Hemisphere-Cylinders at Hypersonic Conditions." AEDC-TDR-63-102 (AD408568), June 1963. See also AIAA Journal. Vol. 2, No. 3, March 1964, pp. 438-444.
4. Cheng, H. K. "Hypersonic Flow with Combined Leading-Edge Bluntness and Boundary-Layer Displacement Effect." CAL Report AF-1285-A-4, August 1960.
5. Lomax, H. and Inouye, M. "Numerical Analysis of Flow Properties about Blunt Bodies Moving at Supersonic Speeds in an Equilibrium Gas." NASA TR-R-204, July 1964.
6. Inouye, M., Rakich, J. V., and Lomax, H. "A Description of Numerical Methods and Computer Programs for Two-Dimensional and Axisymmetric Supersonic Flow over Blunt-Nosed and Flared Bodies." NASA TN D-2970, August 1965.

7. Christensen, D. "An Iterative Viscous-Inviscid Computer Program with Users Manual." USAF RTD-TDR-63-4140, August 1965.
8. Sims, J. L. "Supersonic Flow around Right Circular Cone Tables for Zero Angle of Attack." ABMA Report No. DA-TR-11-60, March 1960.

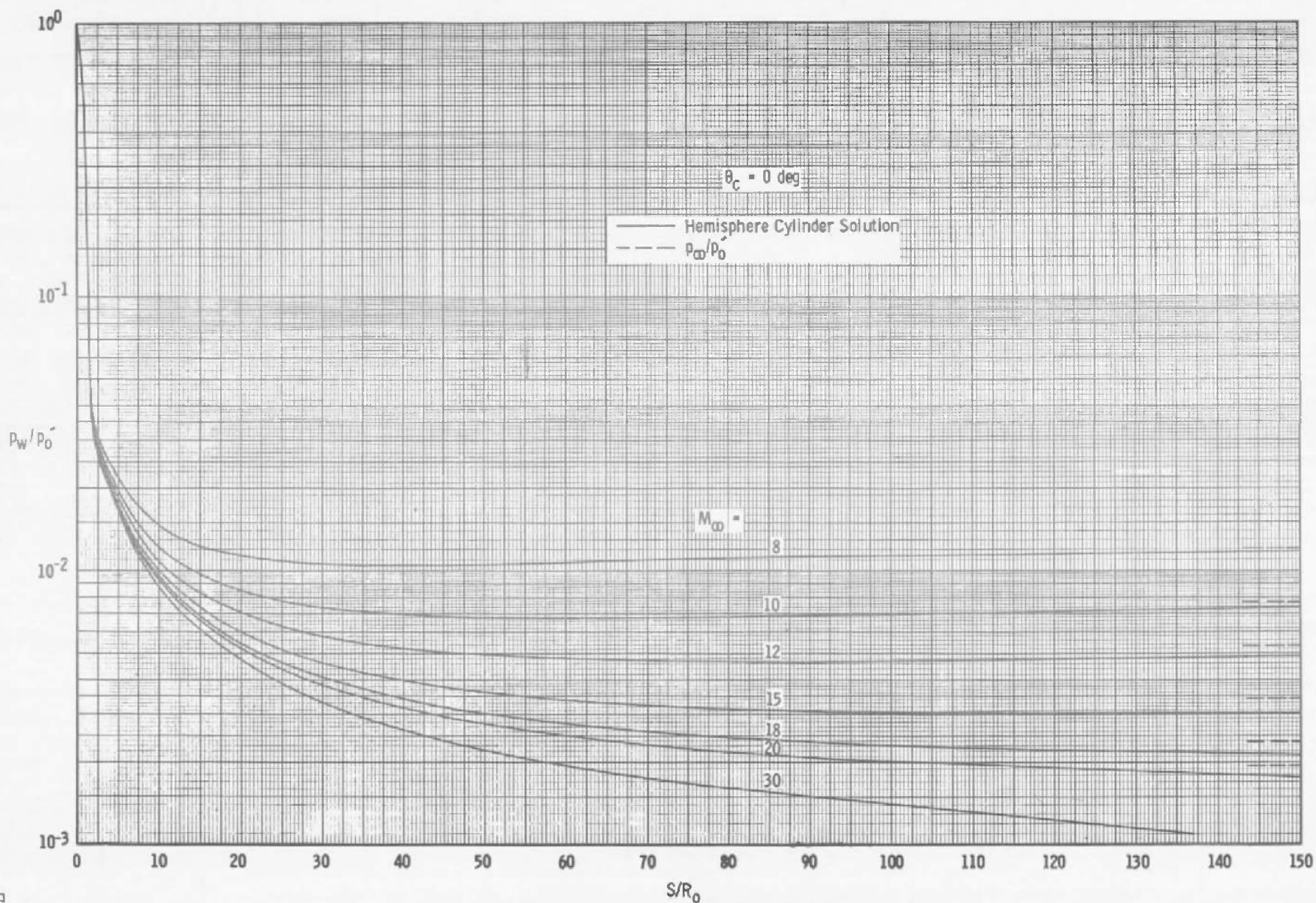


Fig. 1 Surface Pressure Distributions

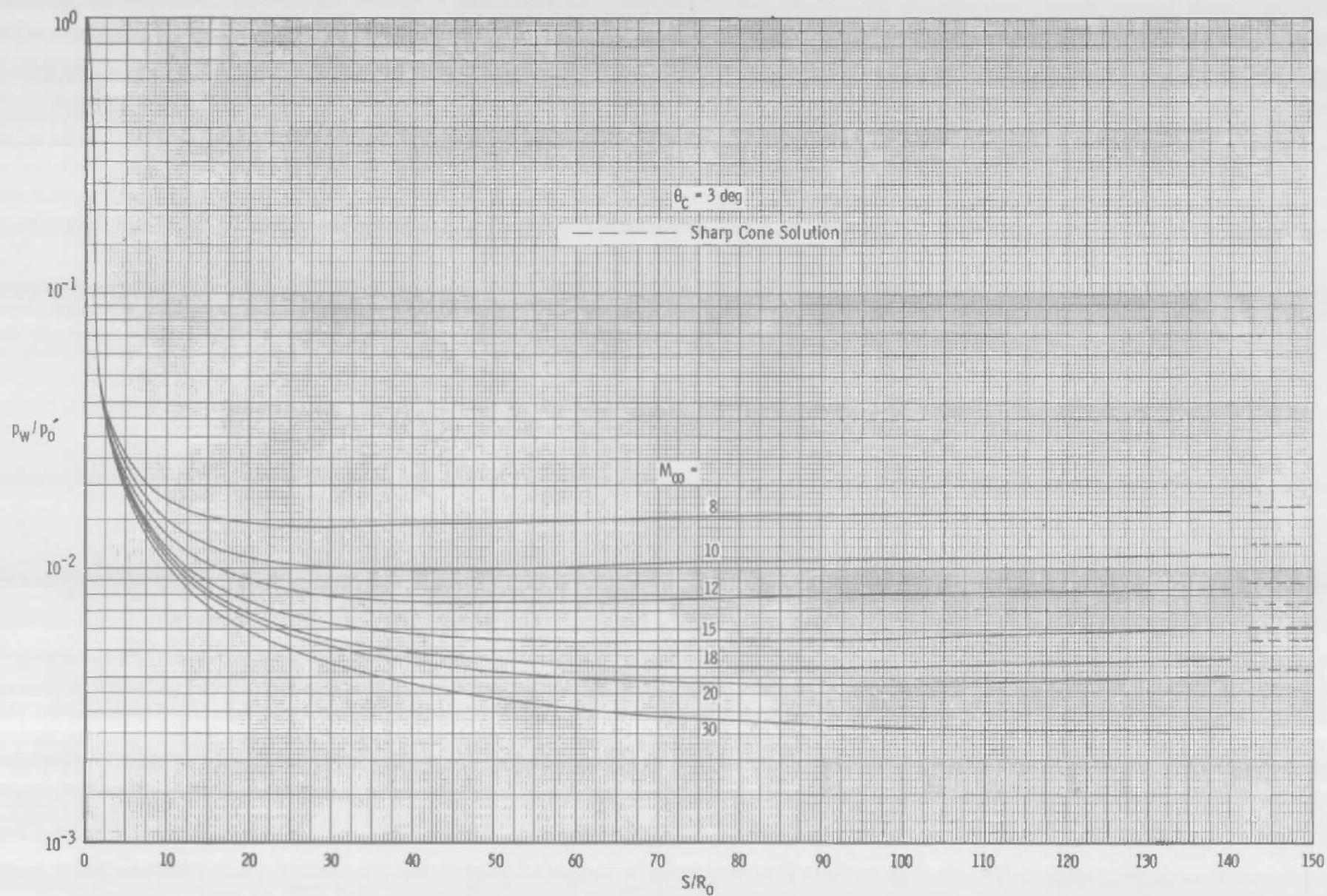


Fig. 1 Continued

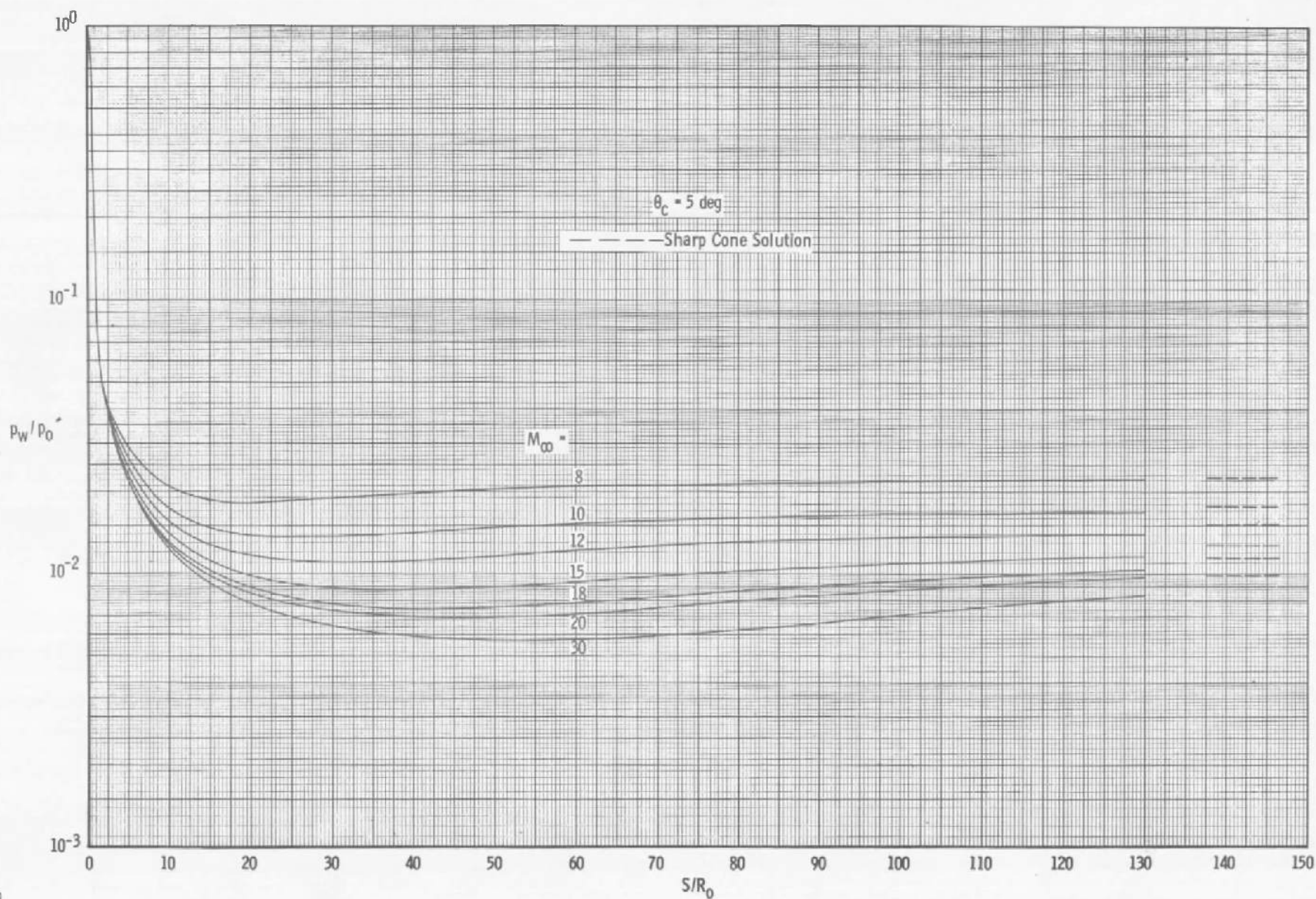


Fig. 1 Continued

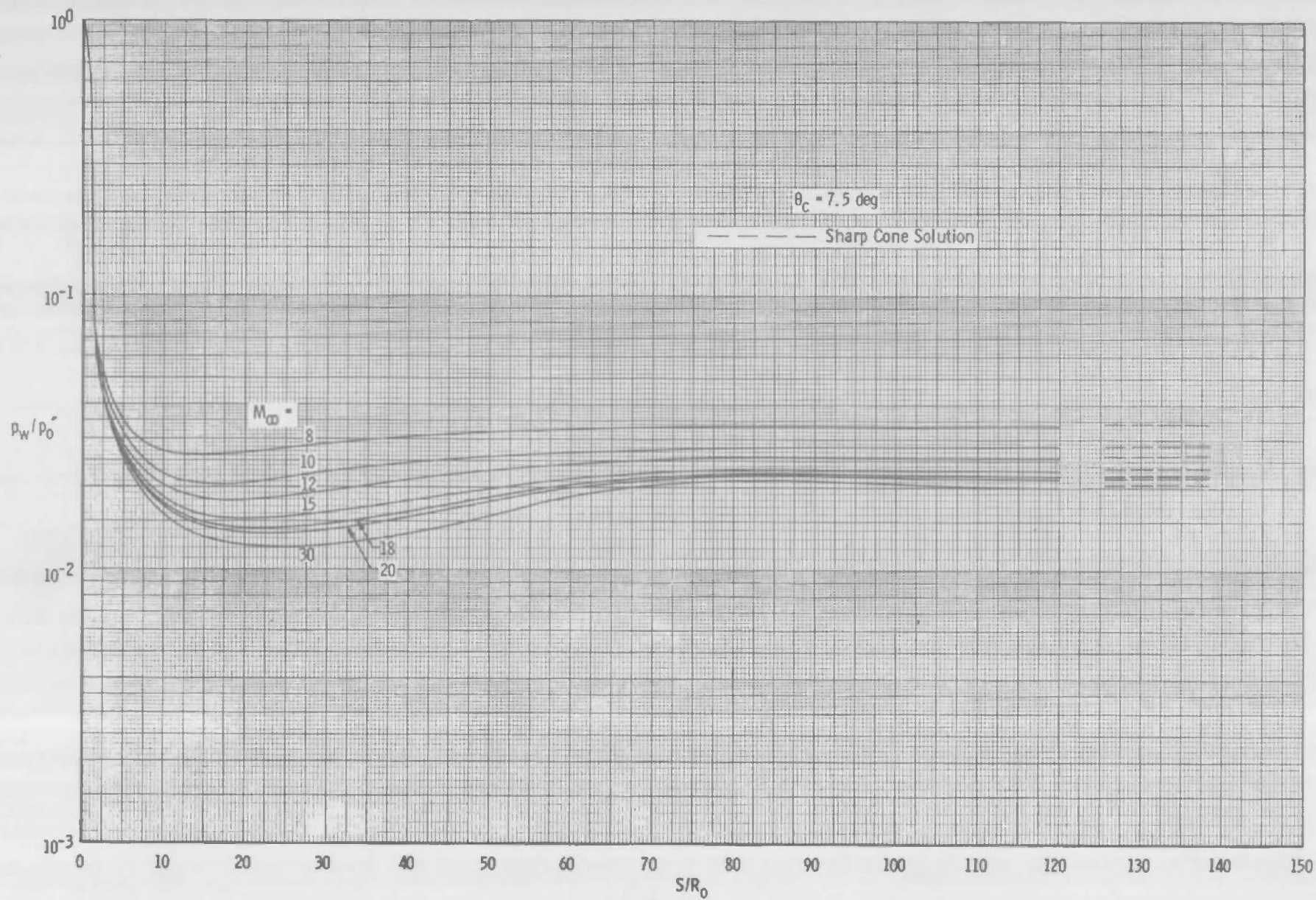


Fig. 1 Continued

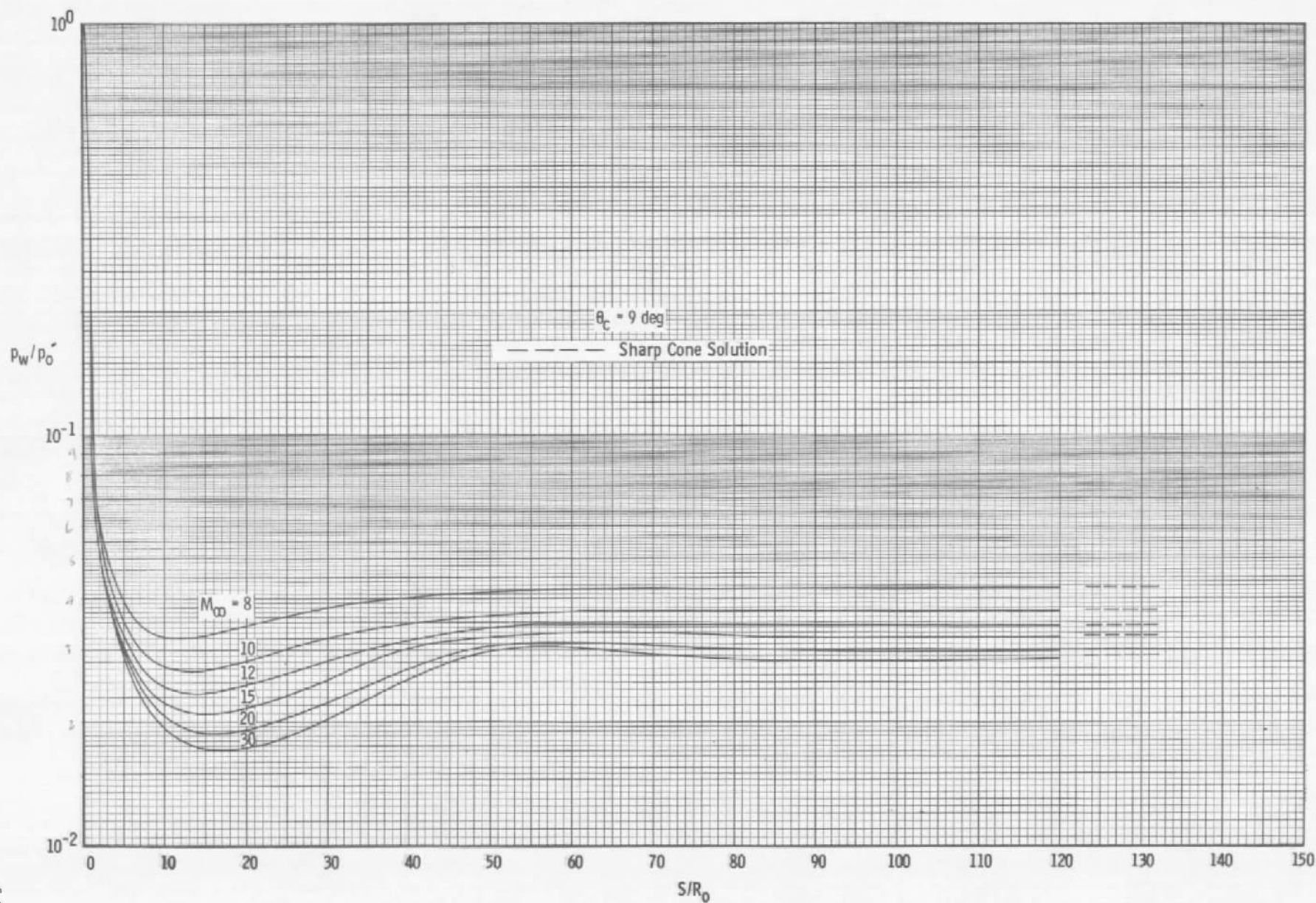


Fig. 1 Continued

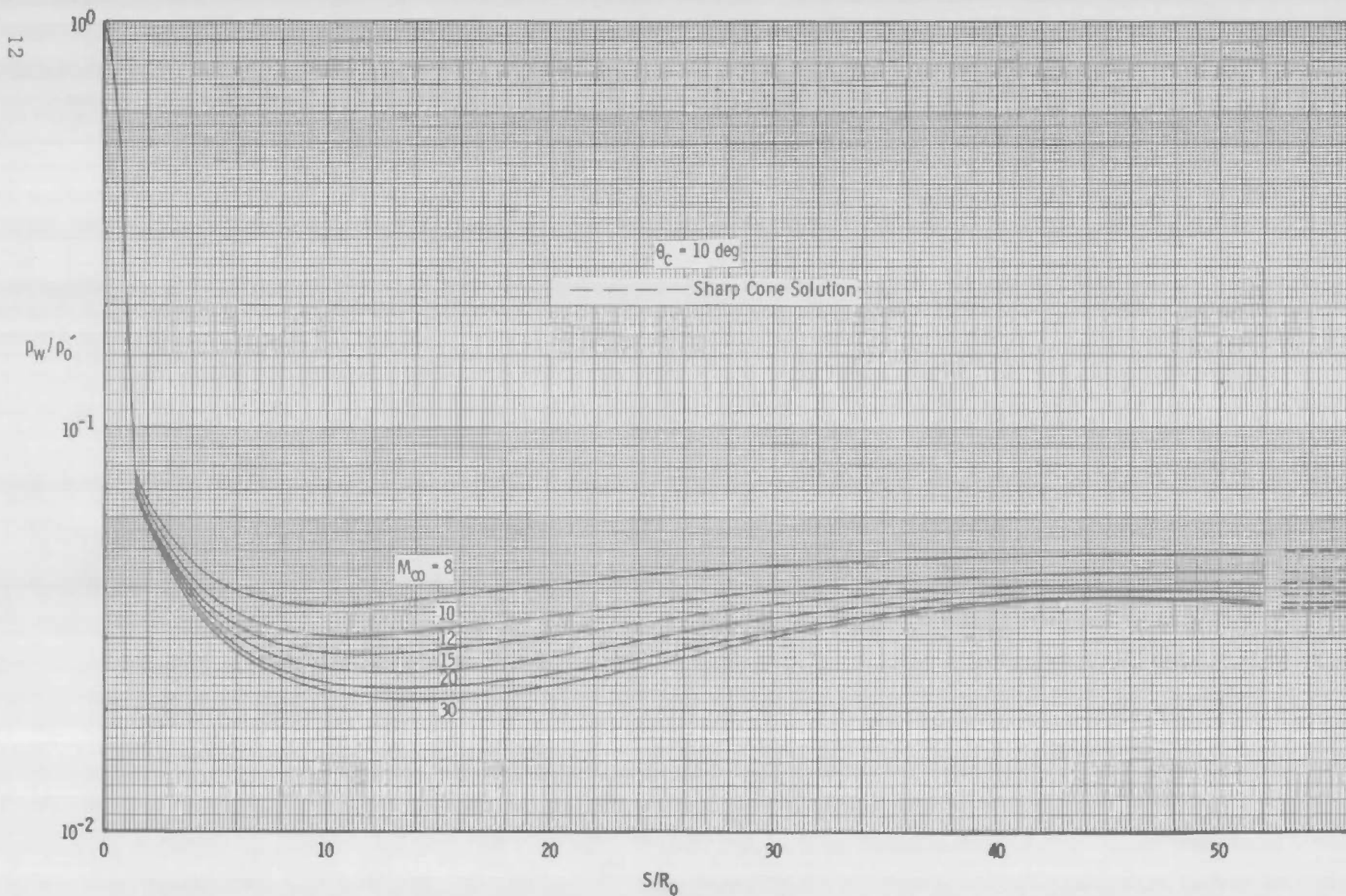


Fig. 1 Continued

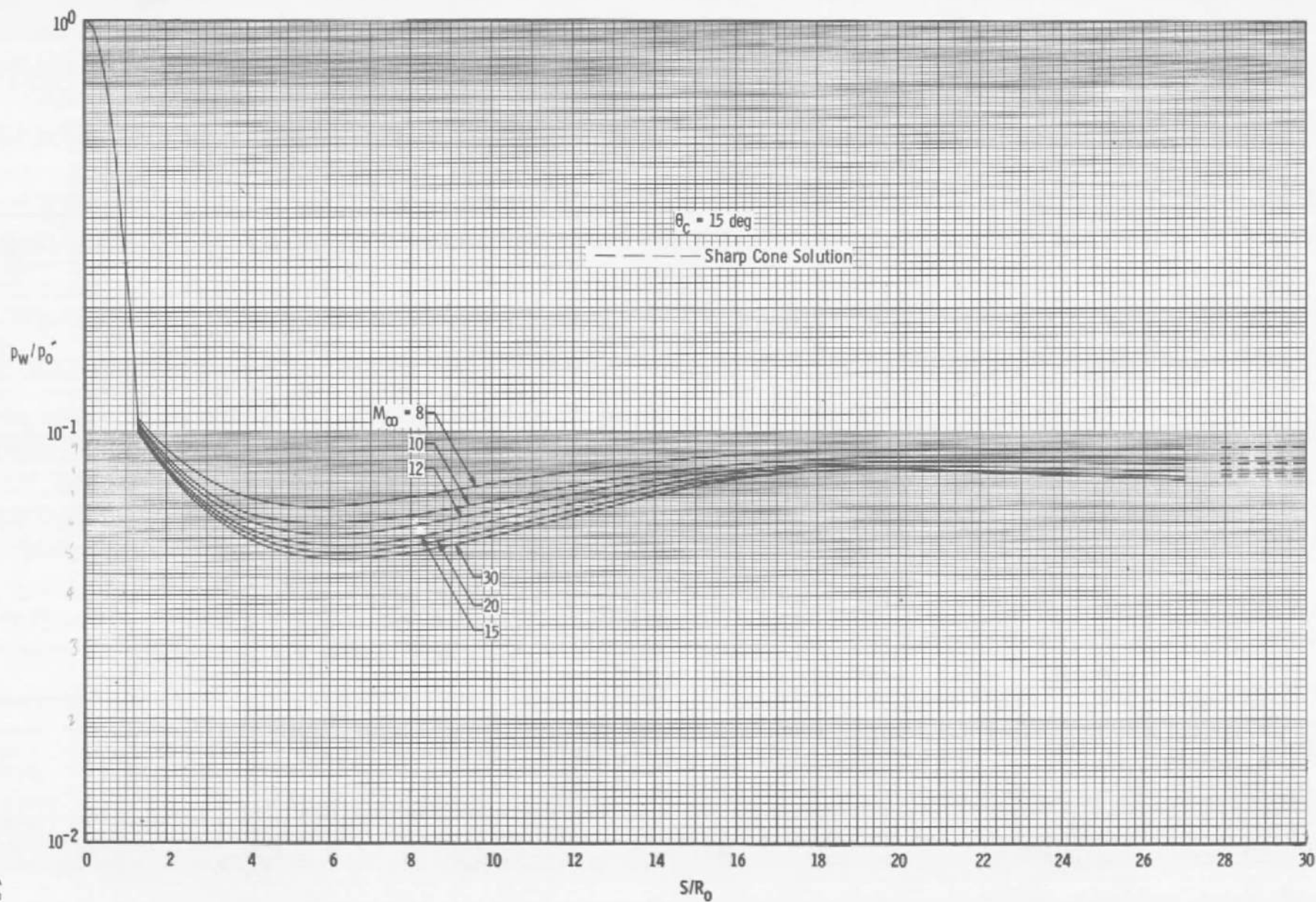


Fig. 1 Continued

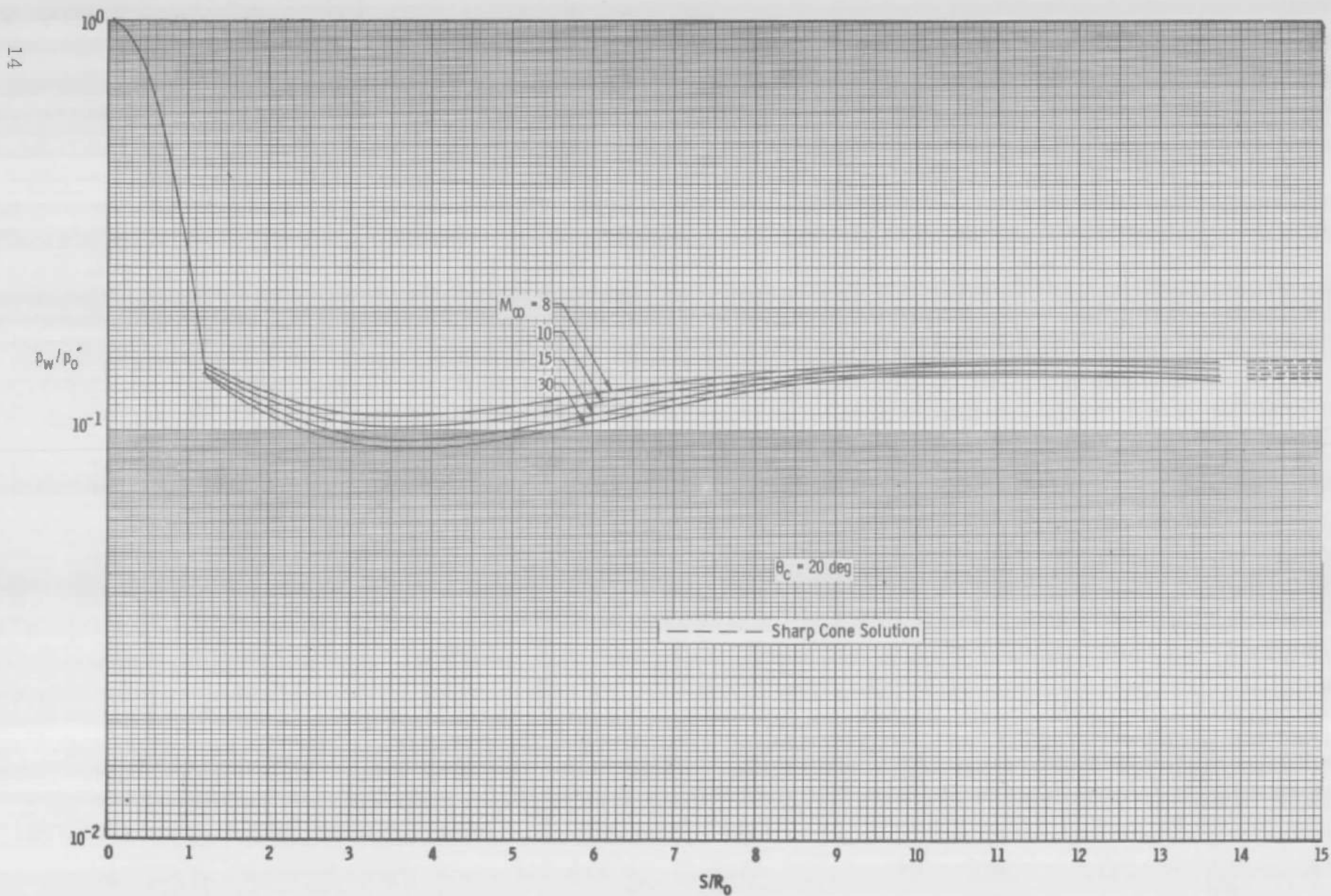


Fig. 1 Continued

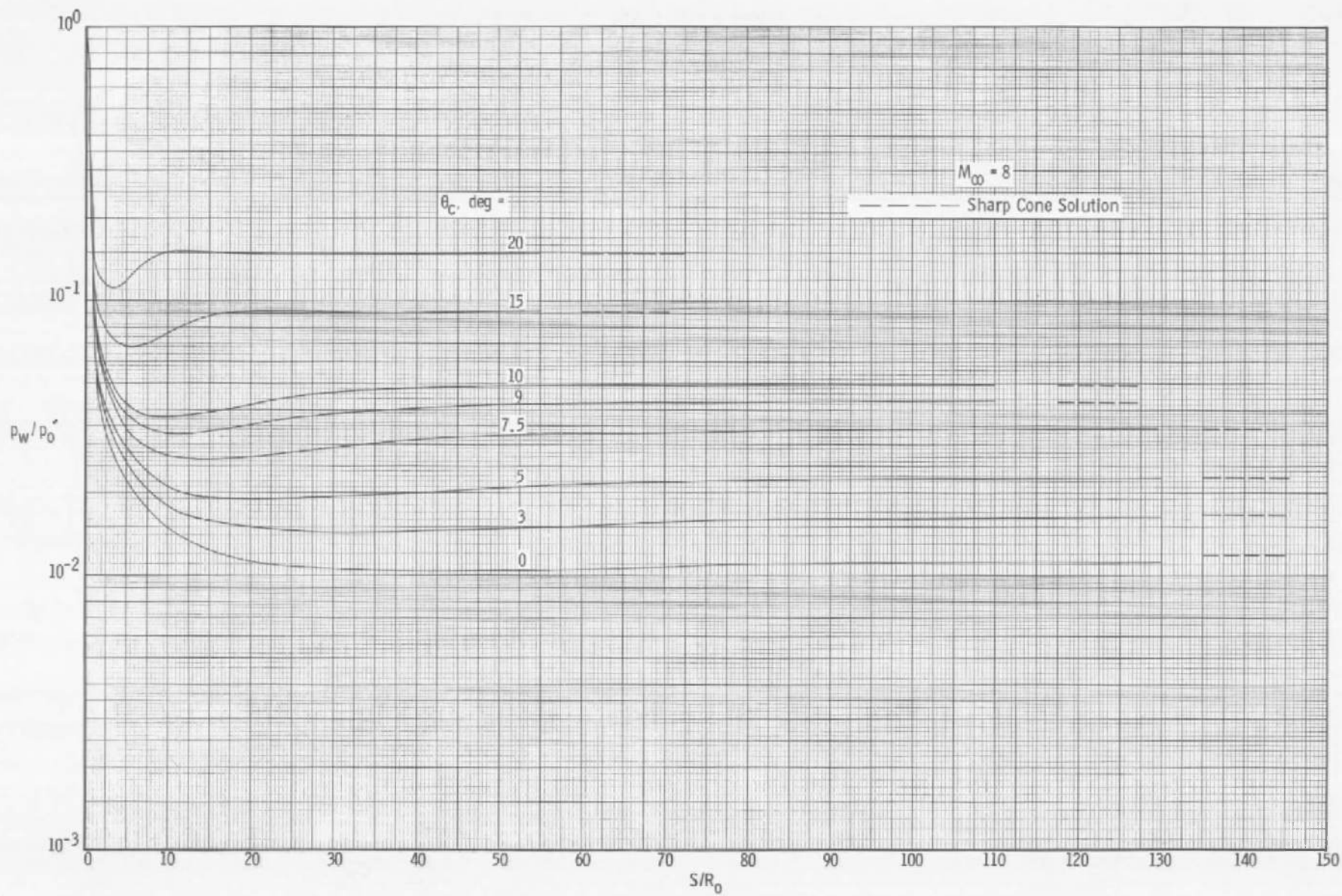


Fig. 1 Continued

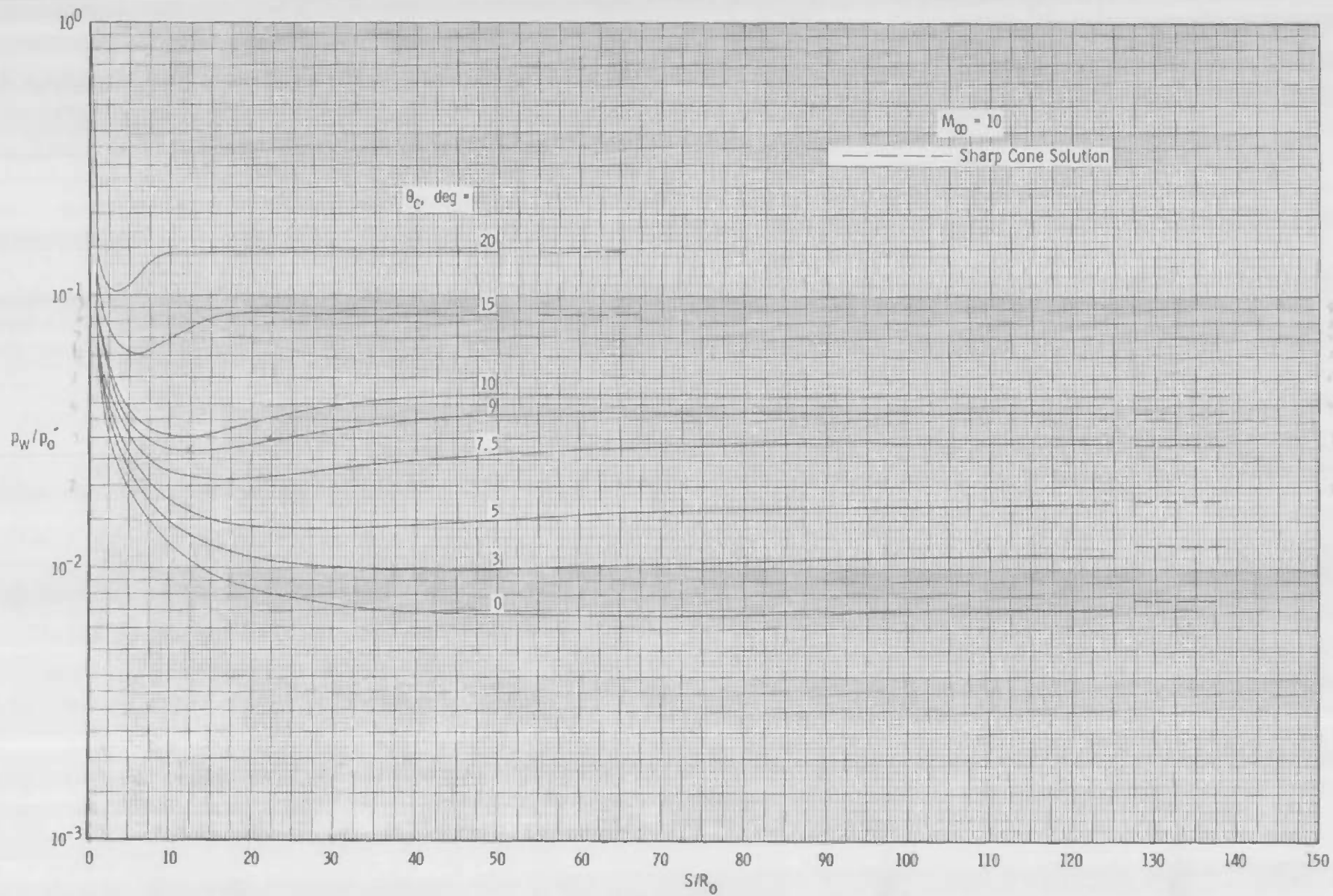


Fig. 1 Continued

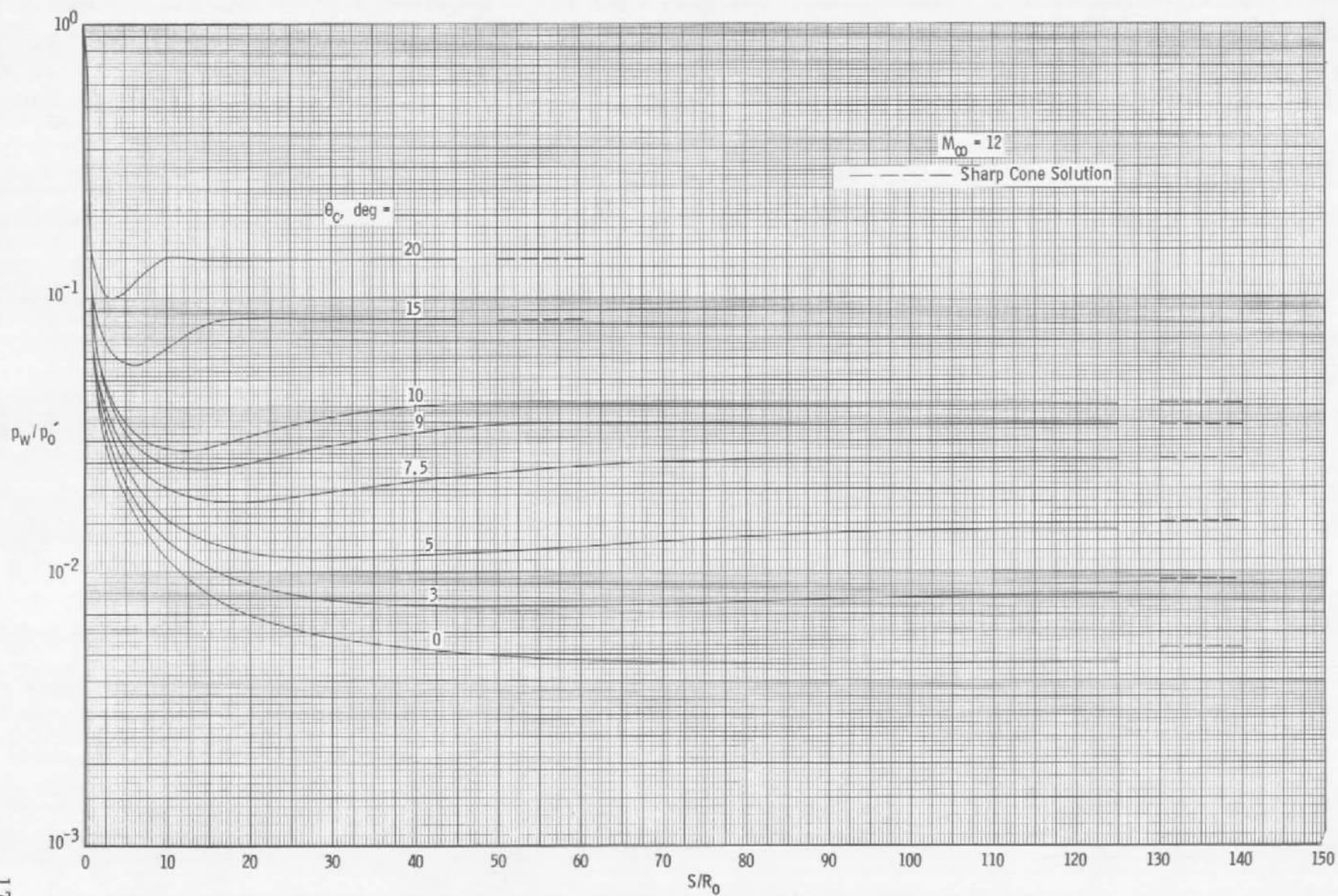


Fig. 1 Continued

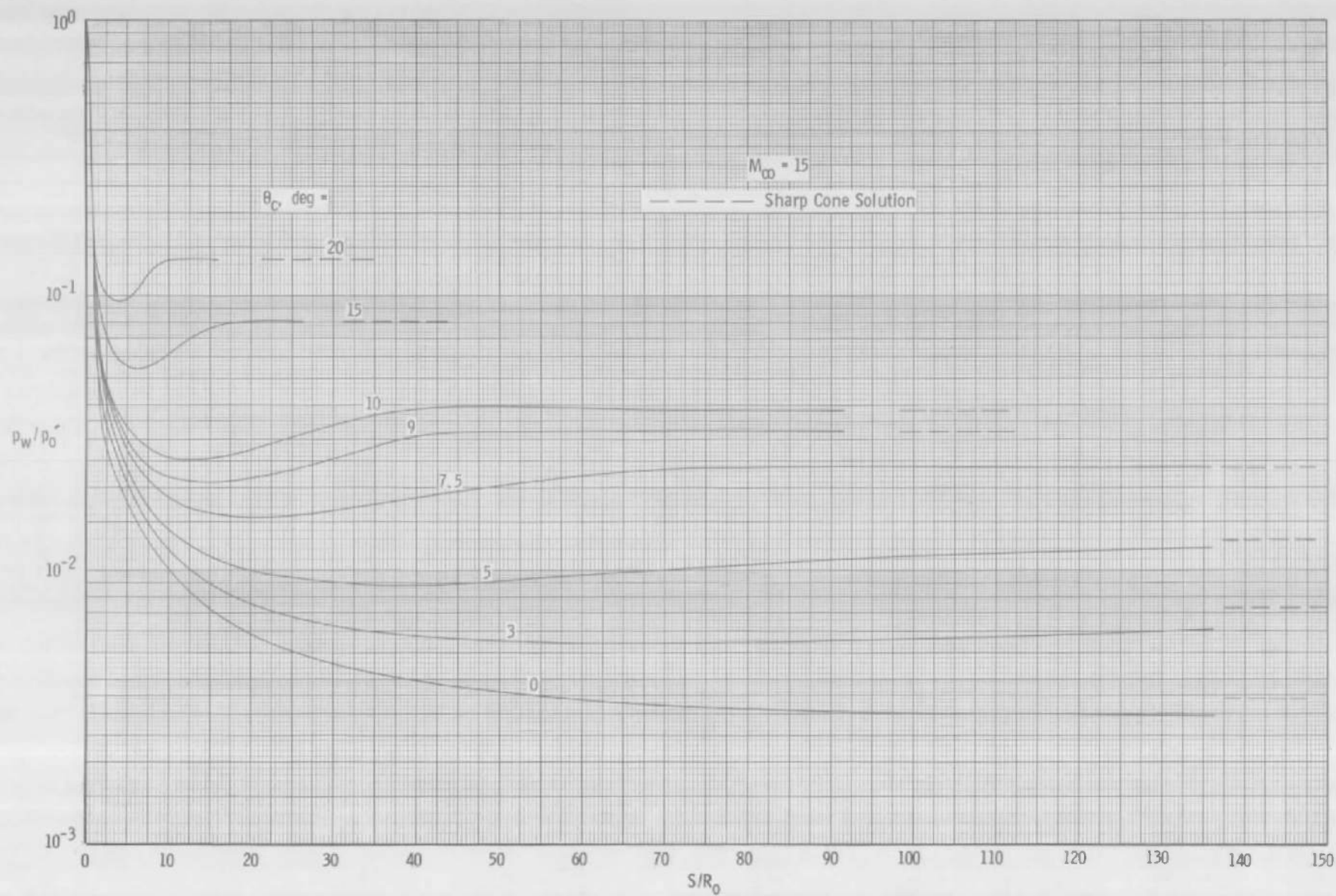


Fig. 1 Continued

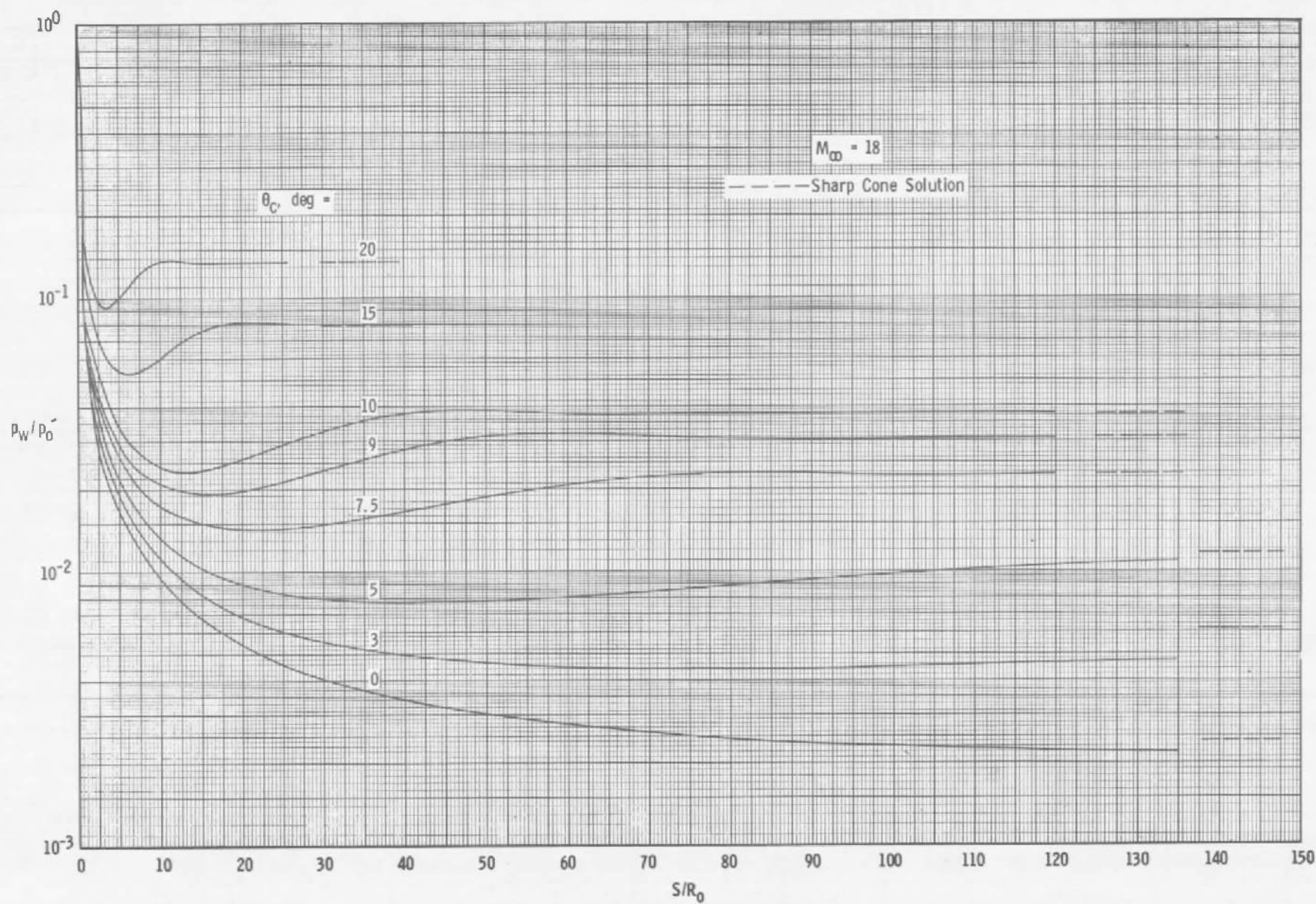


Fig. 1 Continued

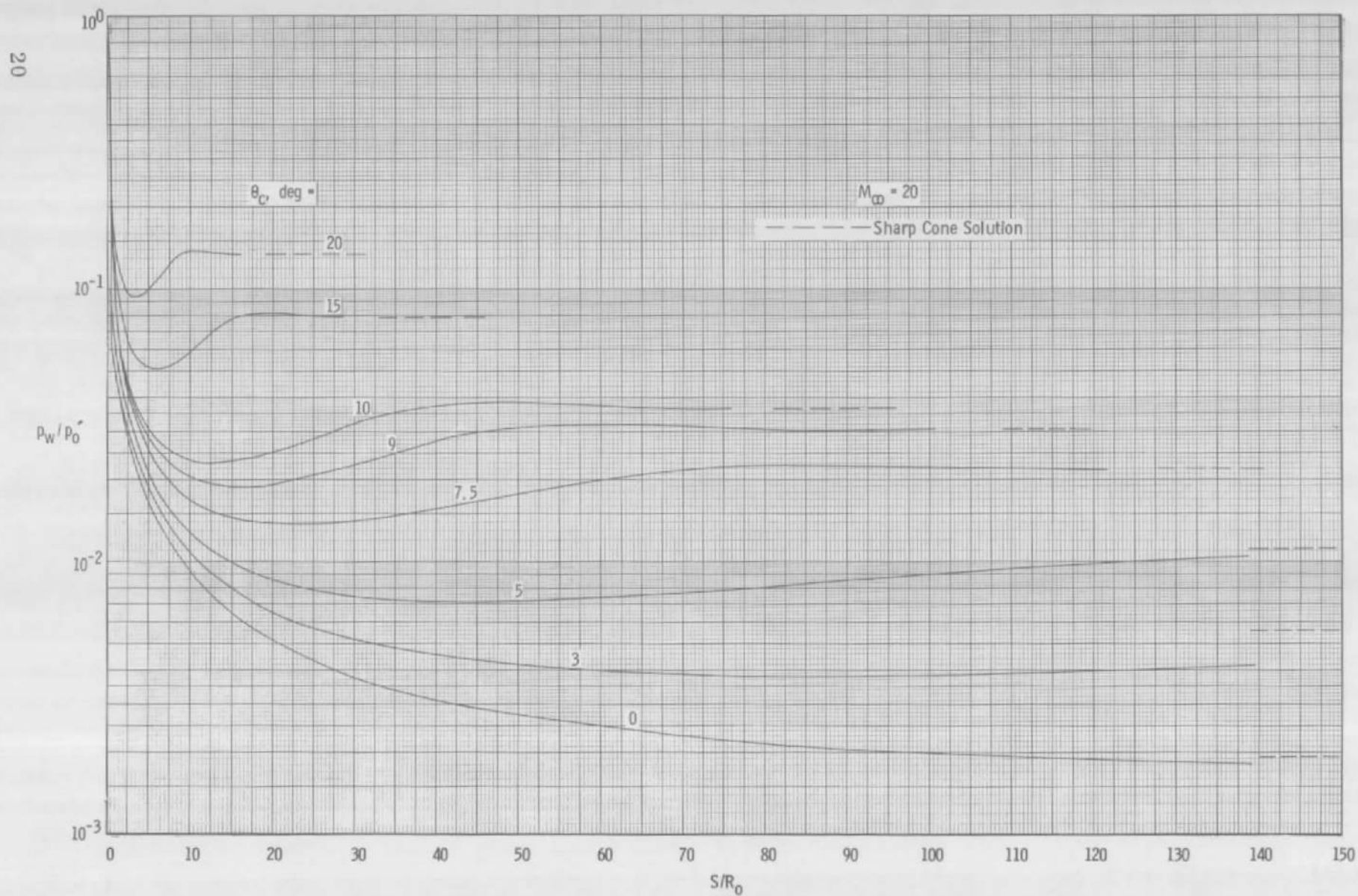


Fig. 1 Continued

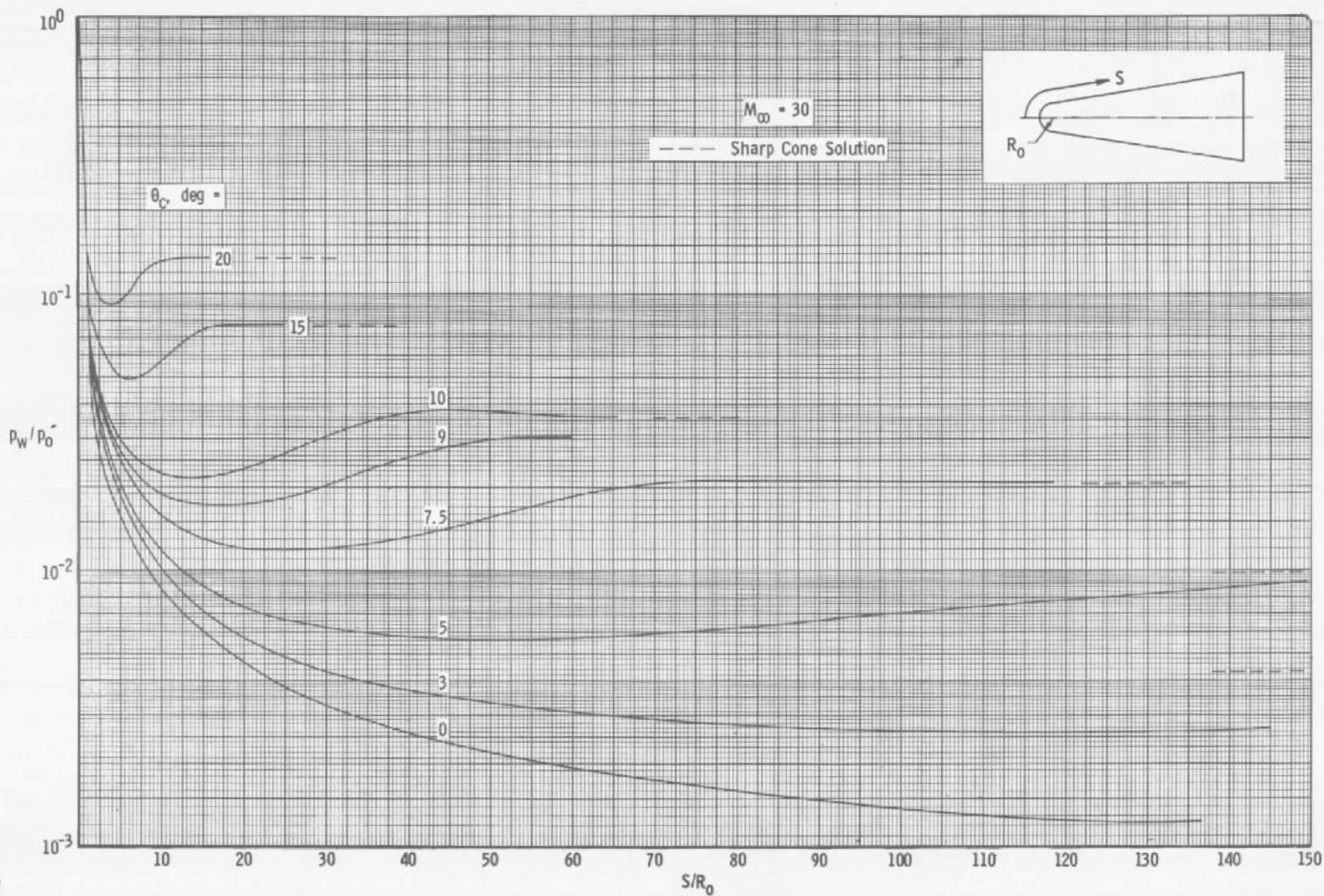


Fig. 1 Concluded

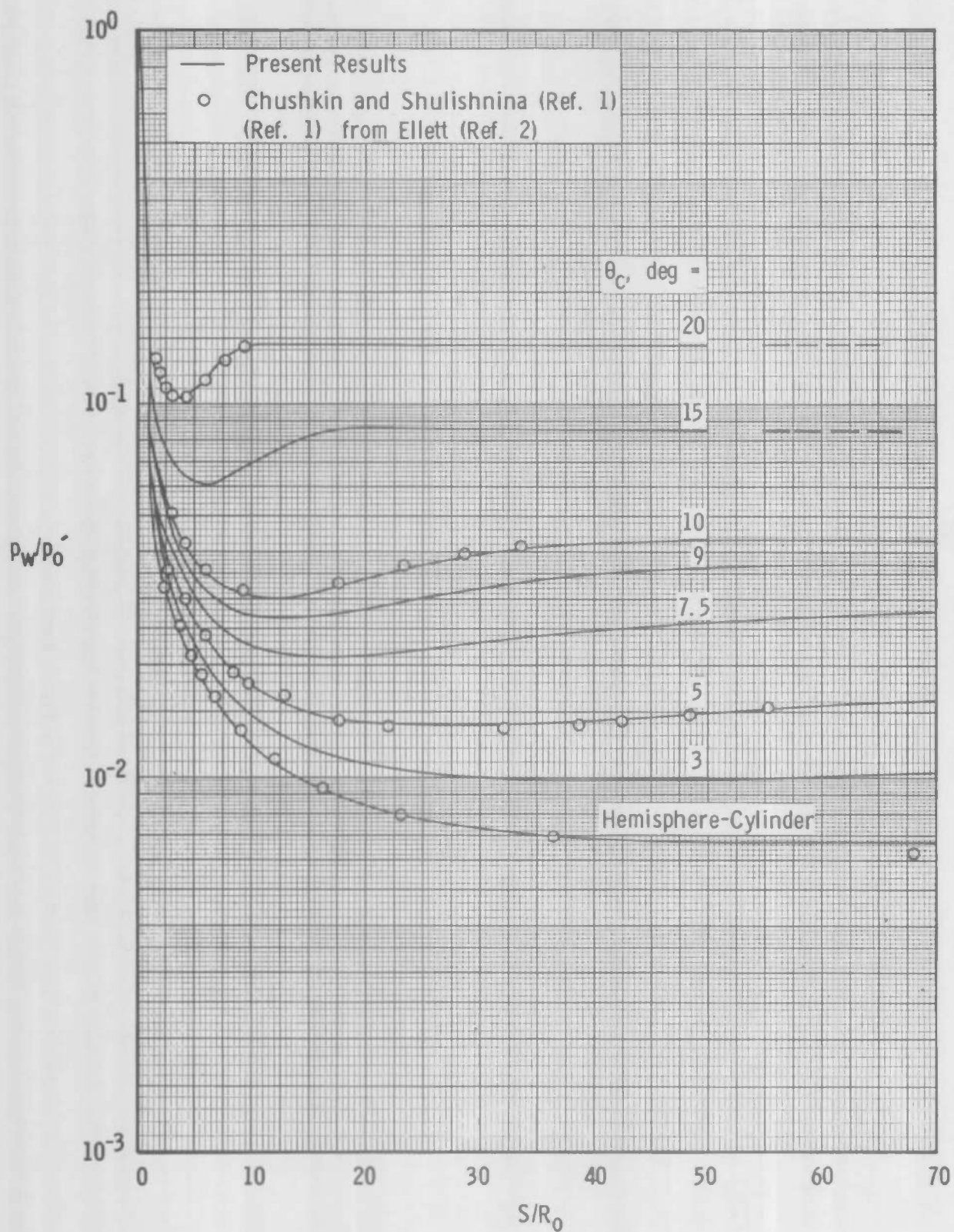


Fig. 2 Comparison of Inviscid, Ideal Gas ($\gamma = 1.4$) Surface Pressure Distributions

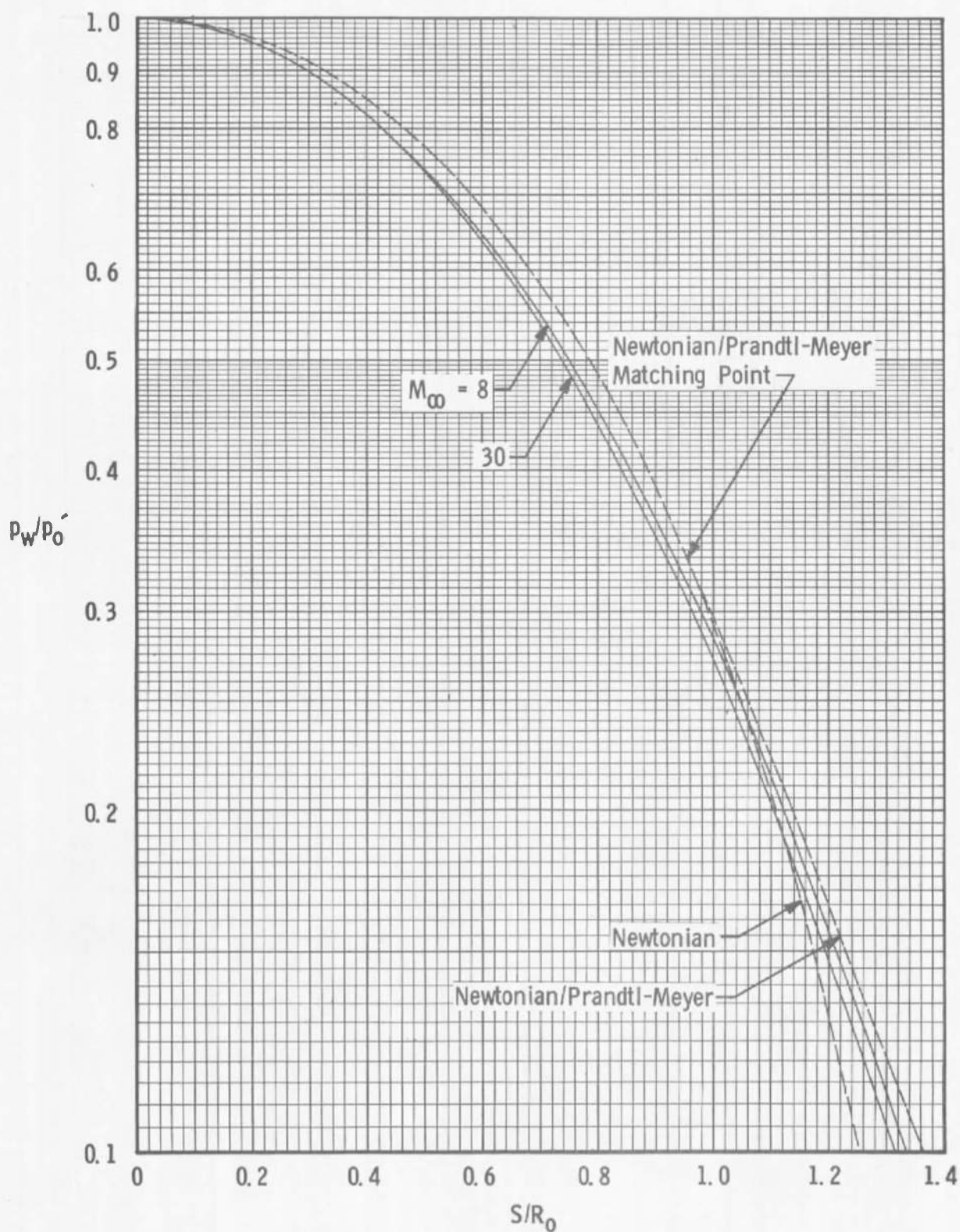


Fig. 3 Pressure Distribution on a Sphere: Comparison of Approximate Theories with the Present Numerical Results

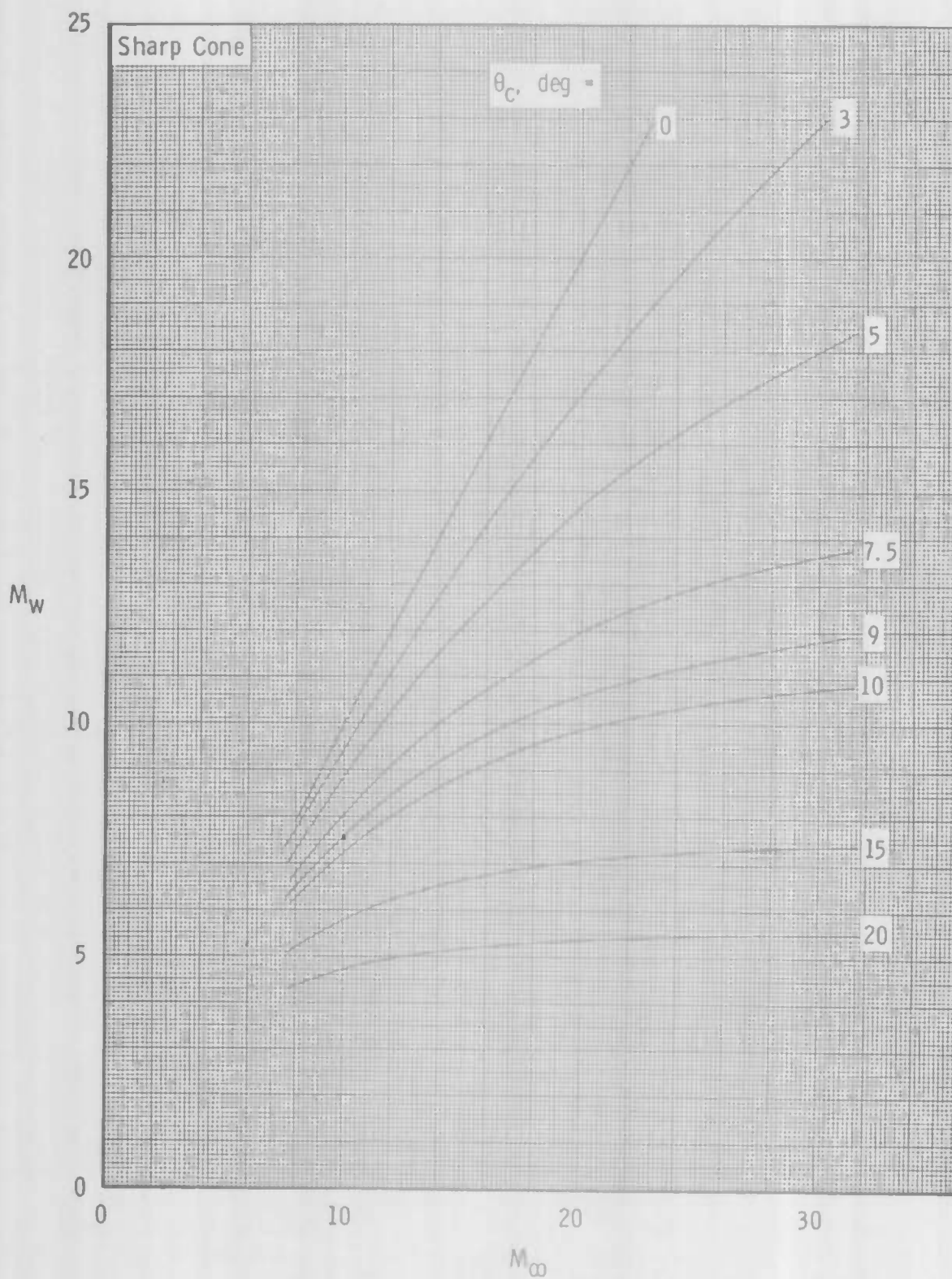


Fig. 4 Surface Mach Number Distributions over Sharp and Blunt Cones

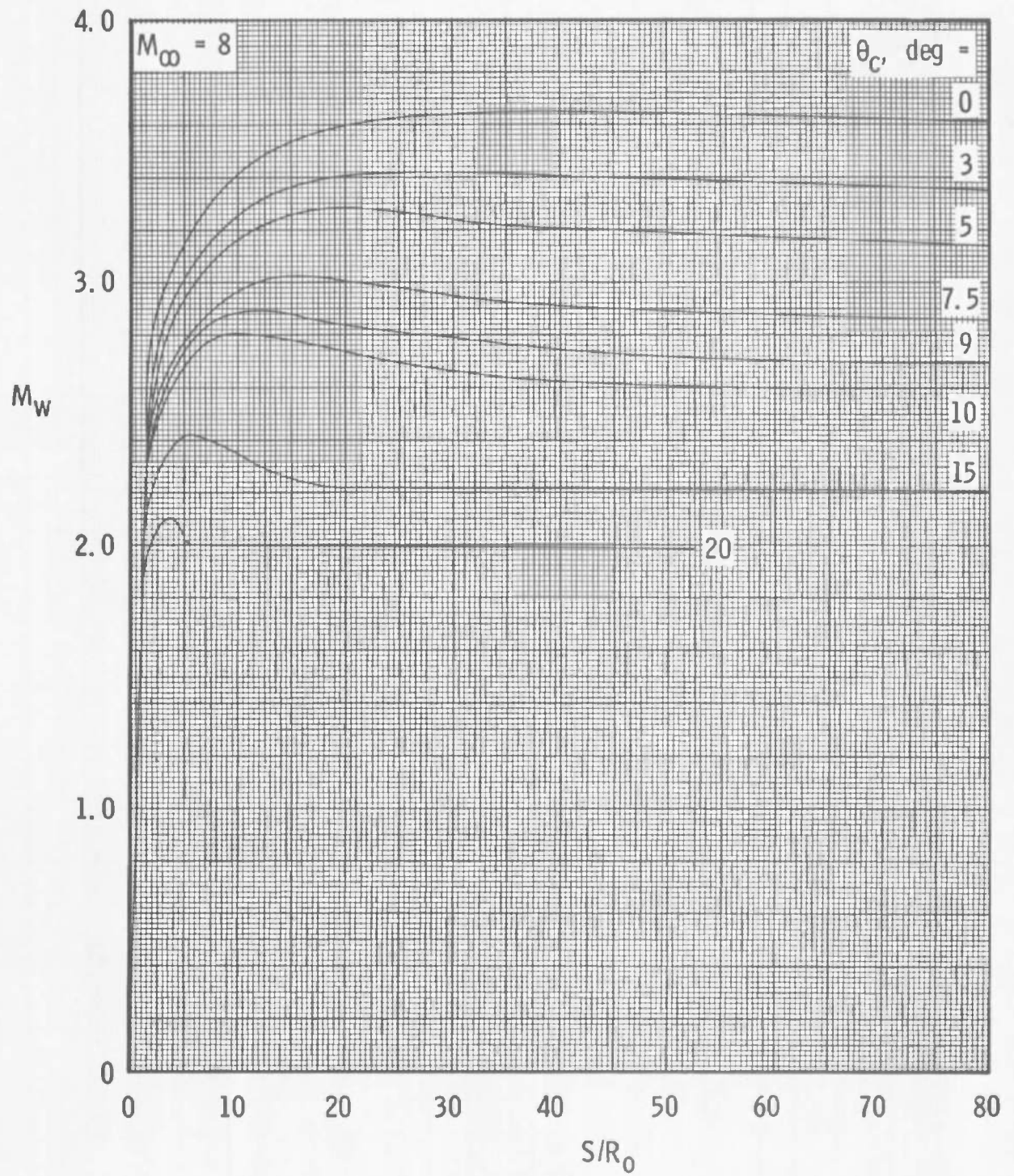


Fig. 4 Continued

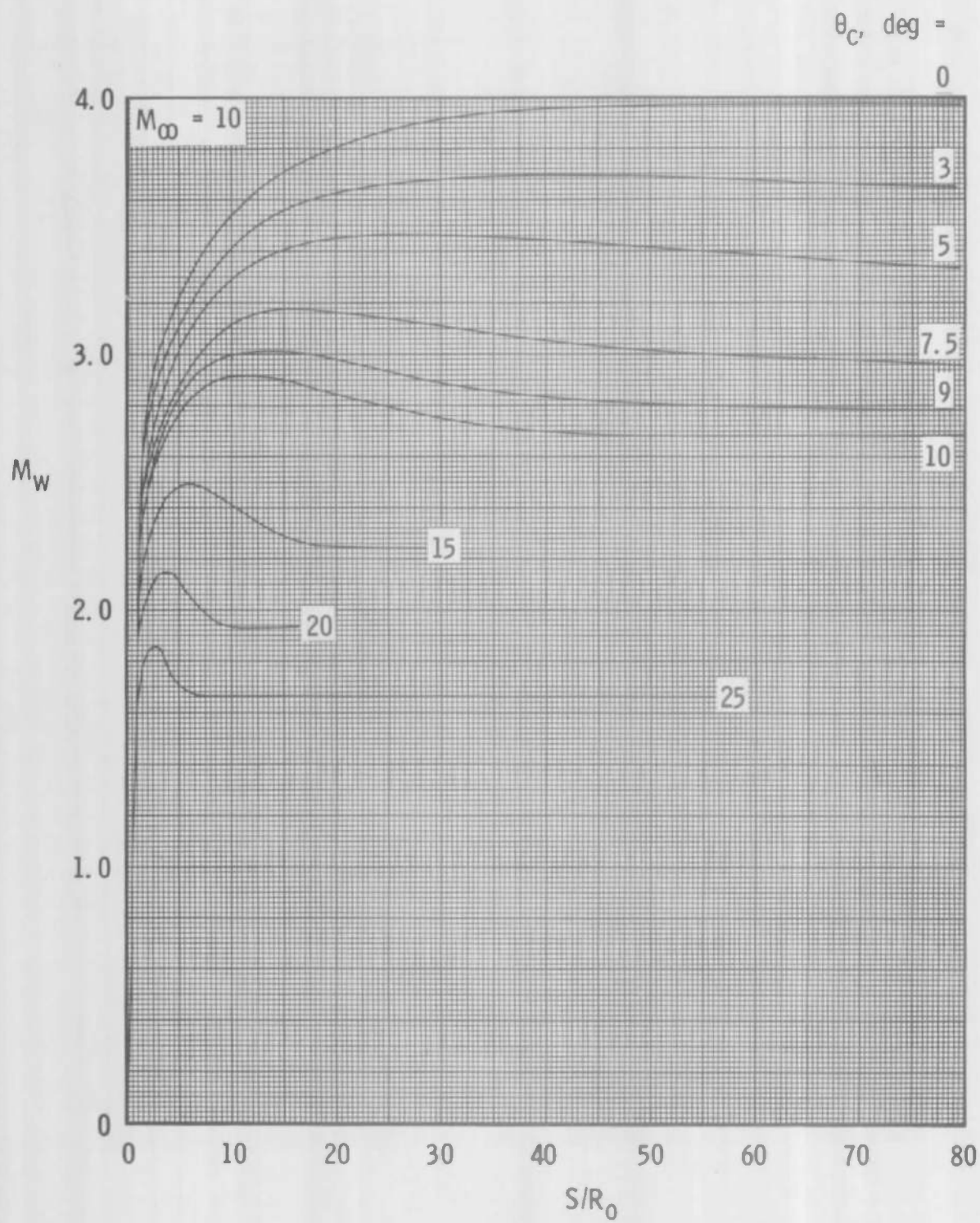


Fig. 4 Continued

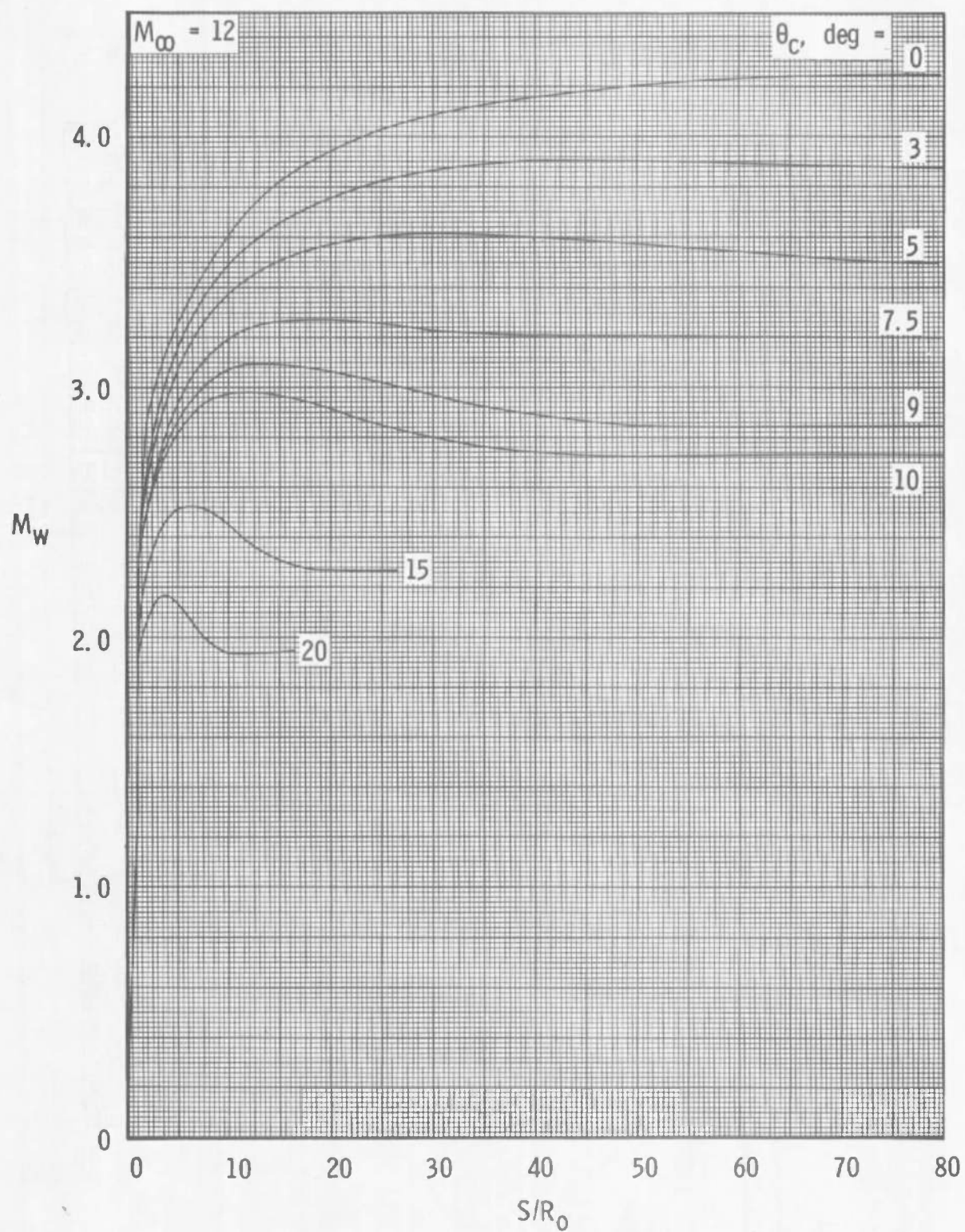


Fig. 4 Continued

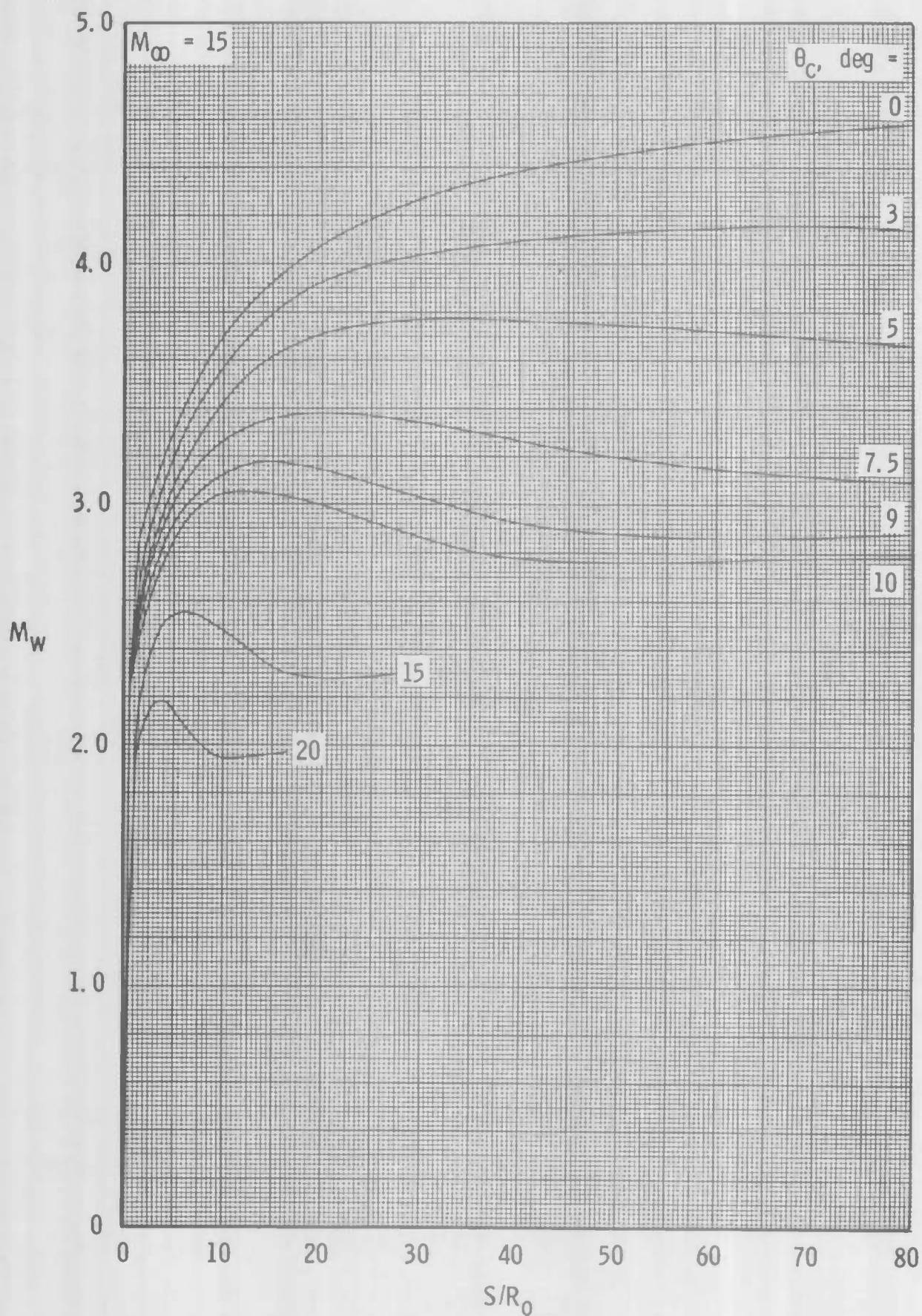


Fig. 4 Continued

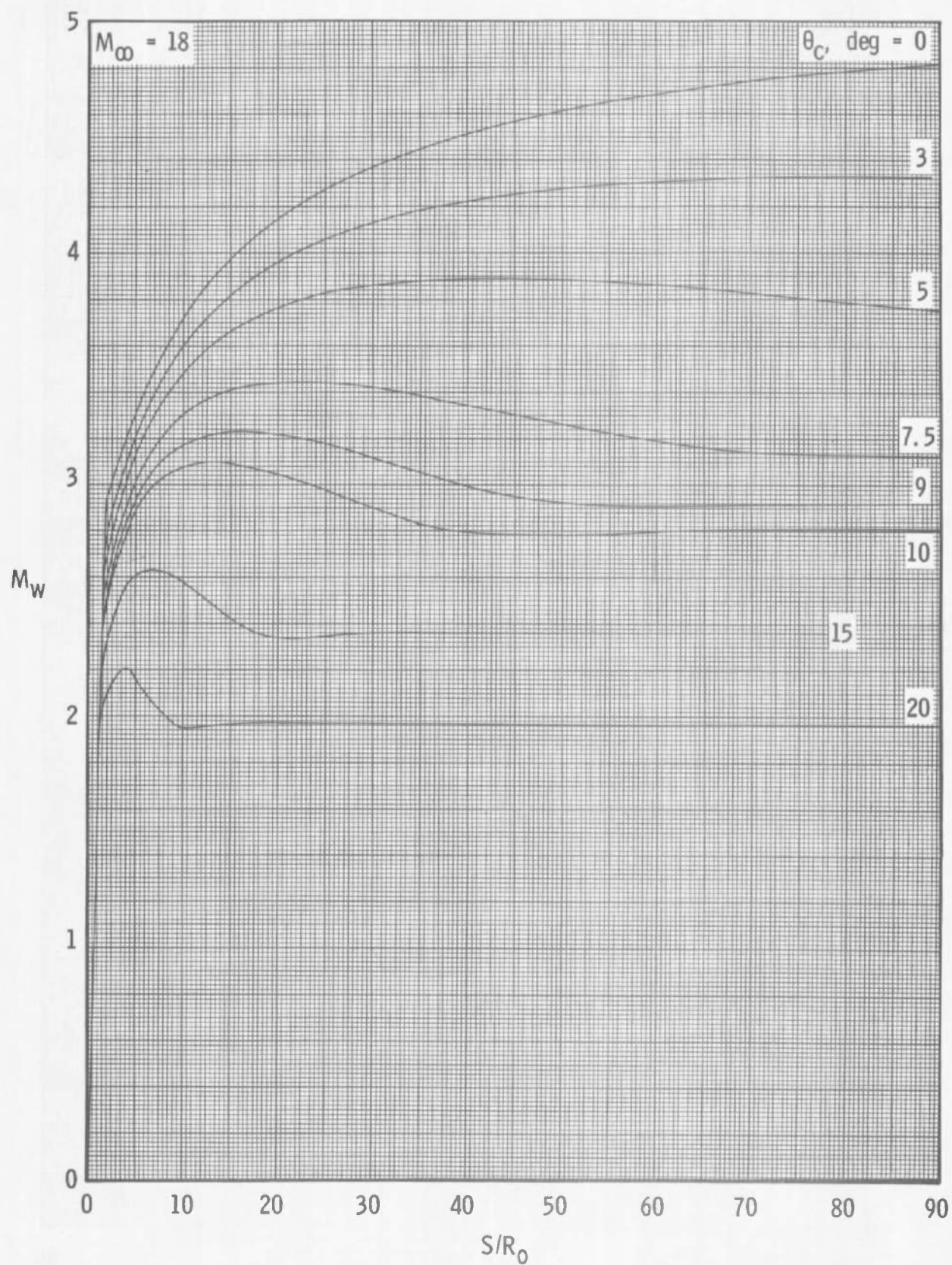


Fig. 4 Continued

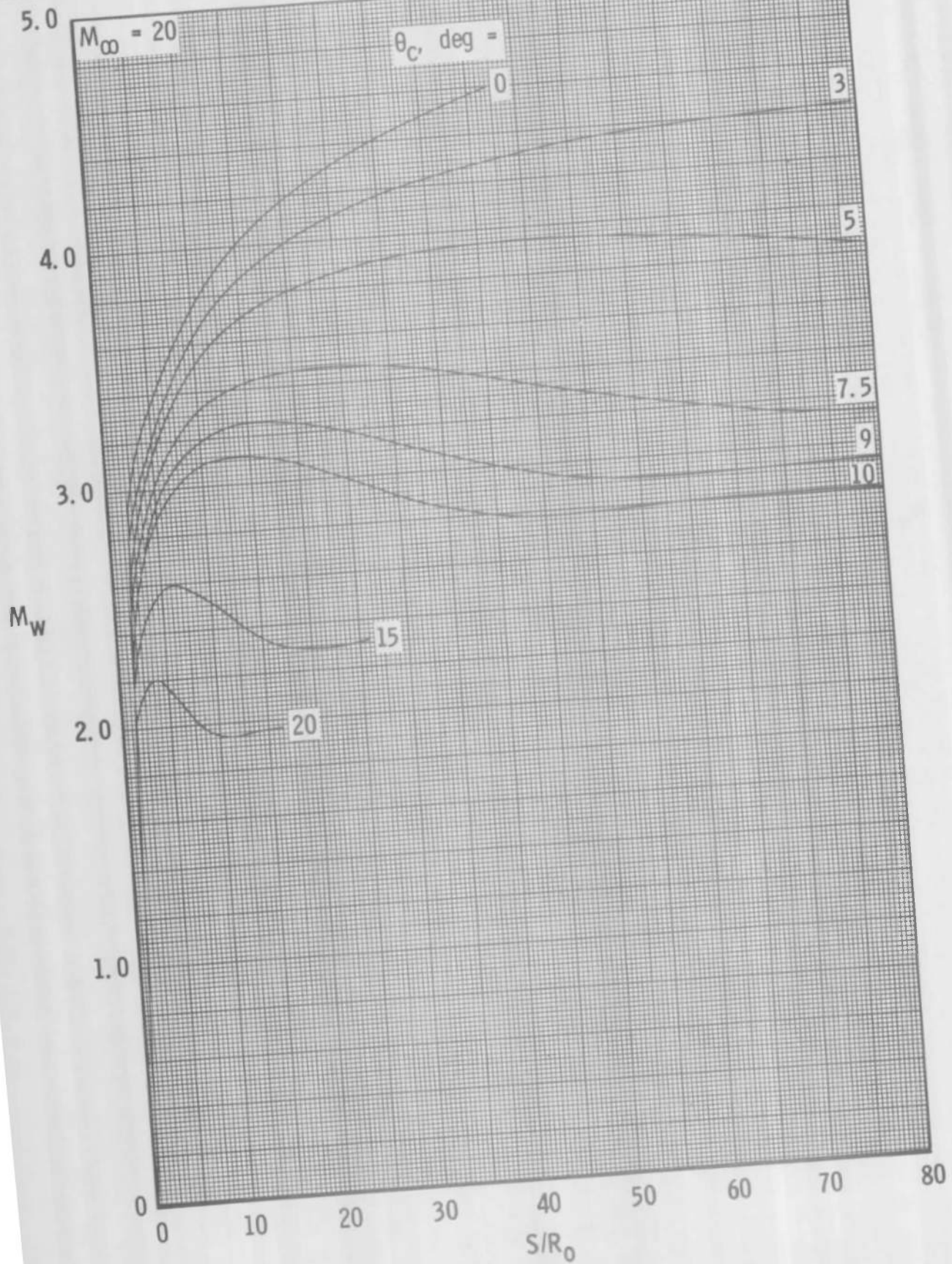


Fig. 4 Continued

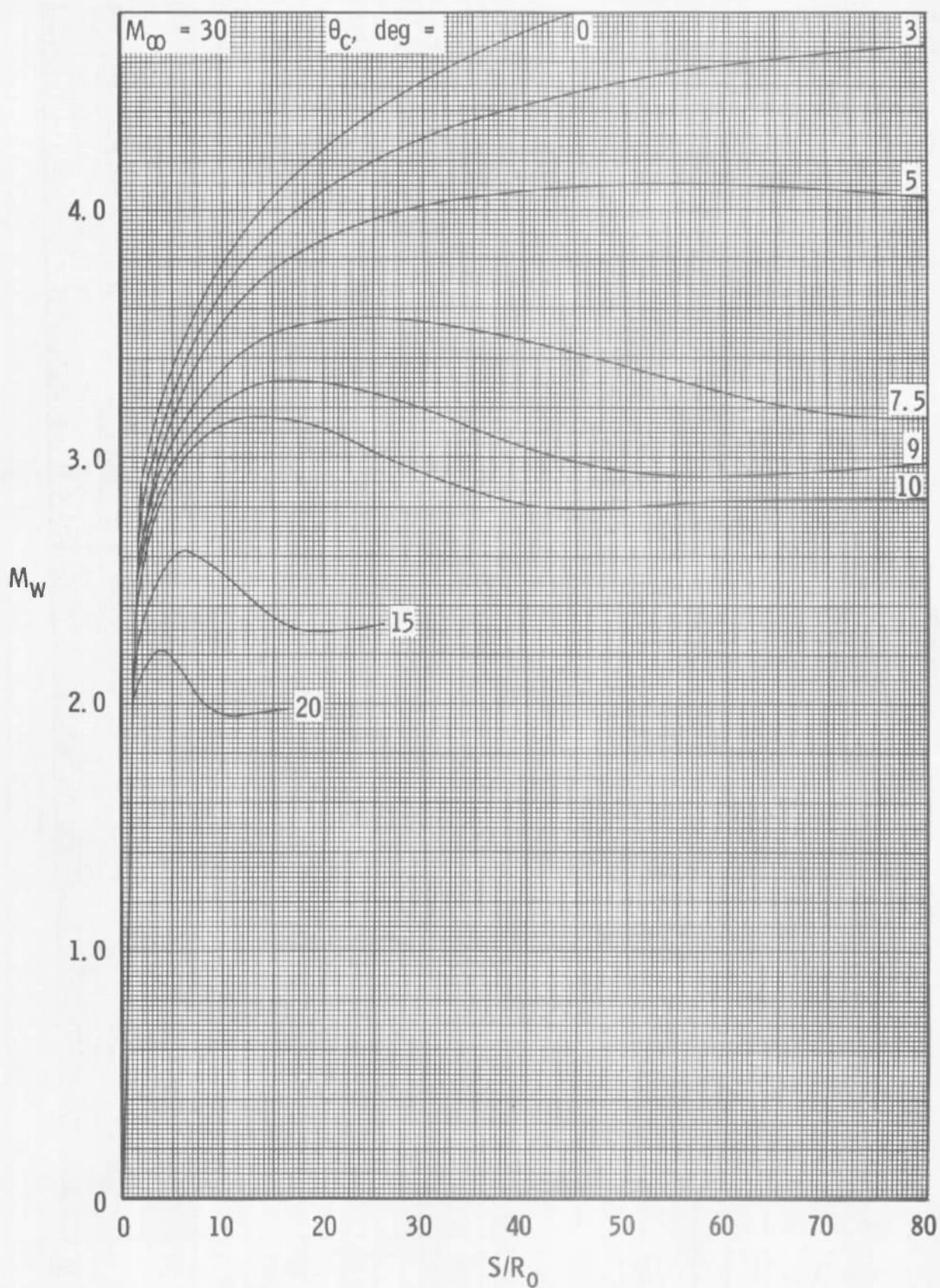


Fig. 4 Concluded

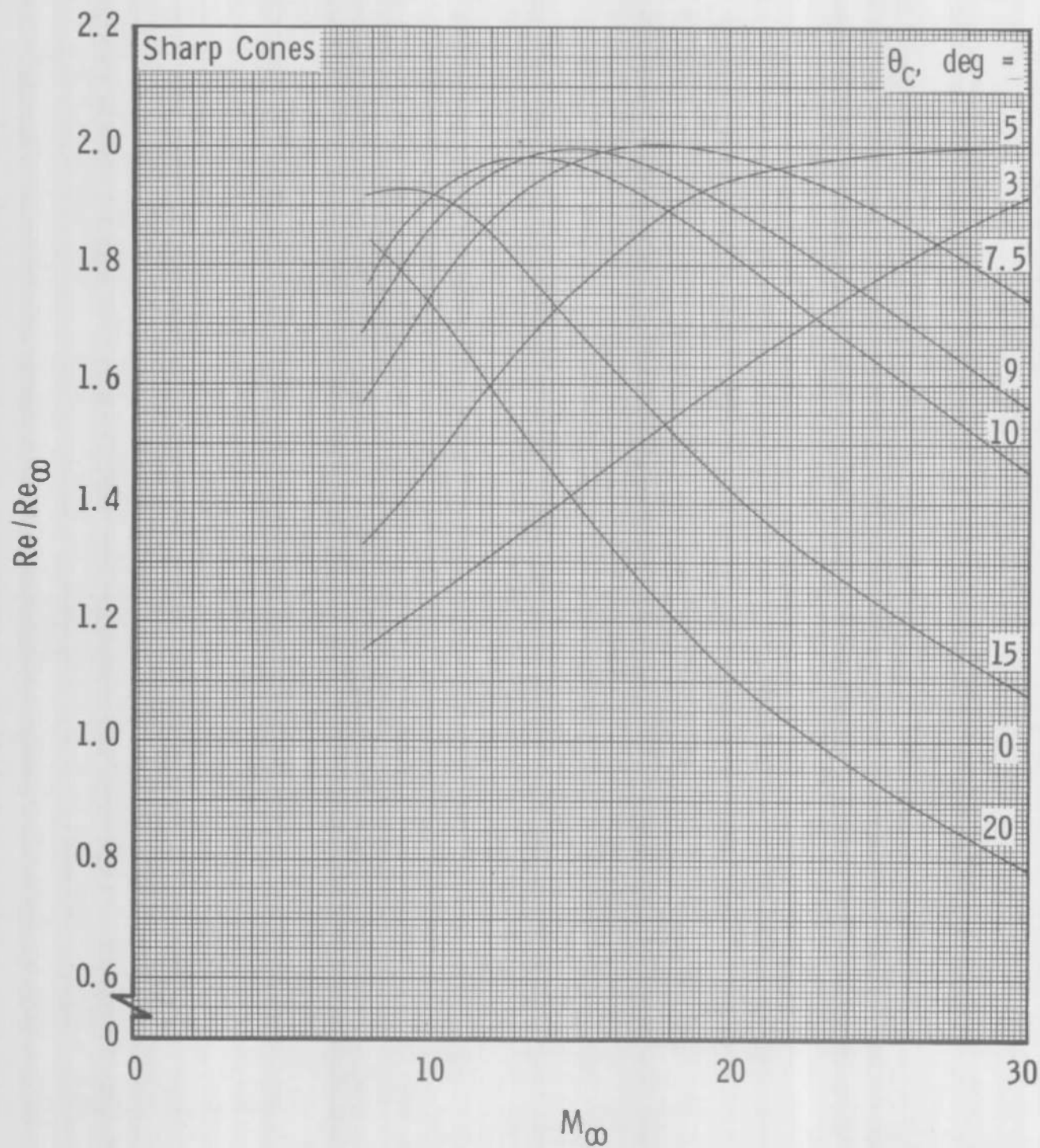


Fig. 5 Surface-to-Free-Stream Reynolds Number Ratio for Sharp and Blunt Cones

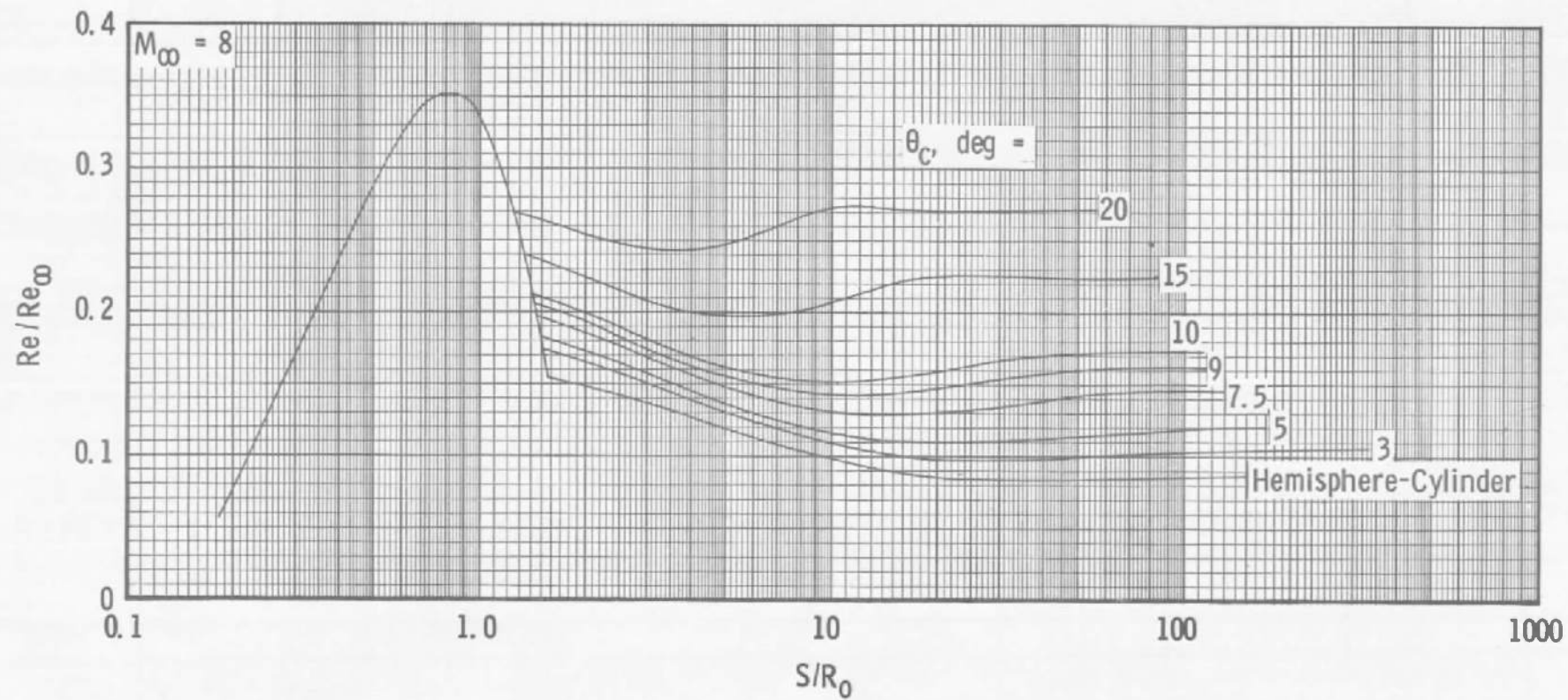


Fig. 5 Continued

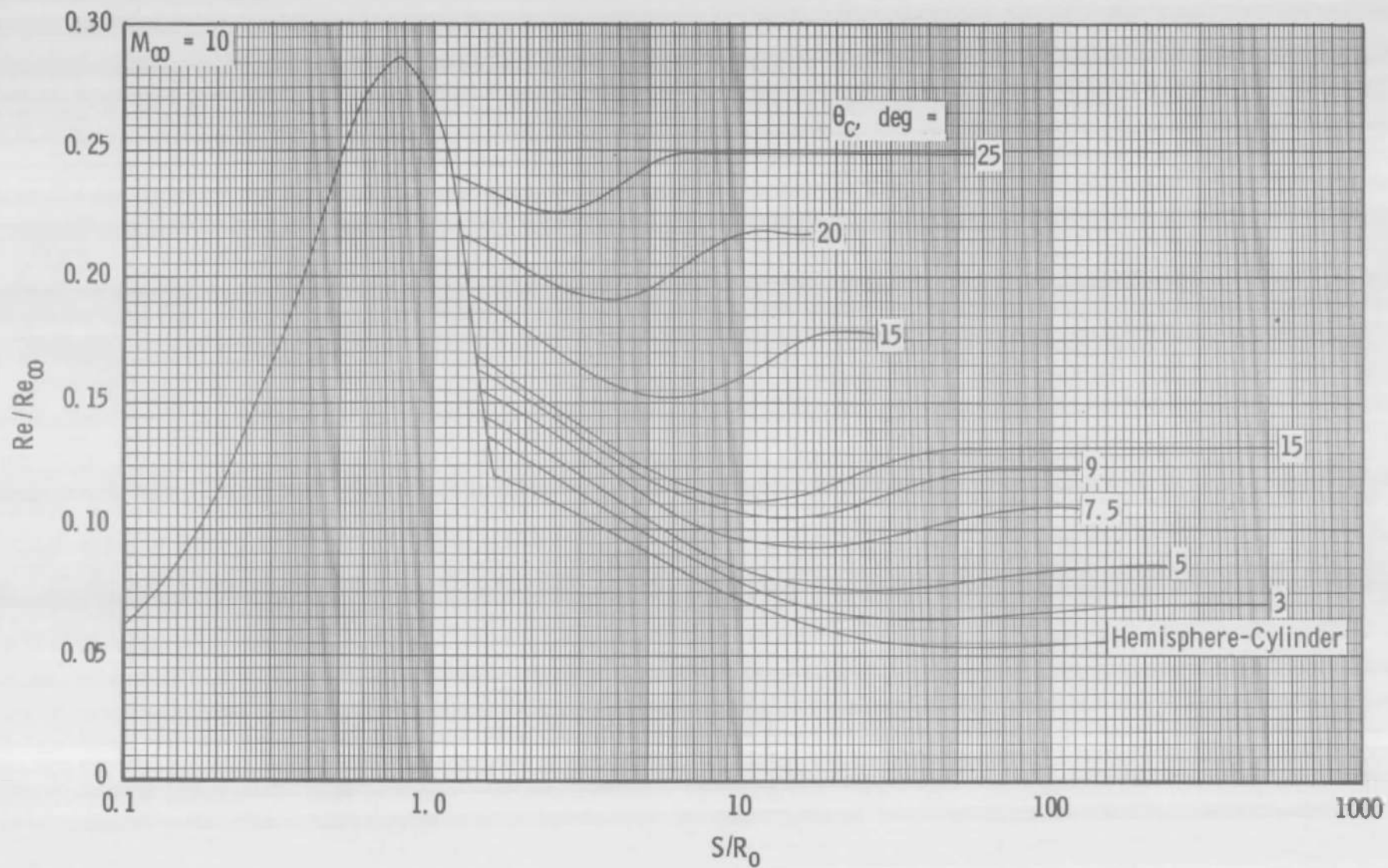


Fig. 5 Continued

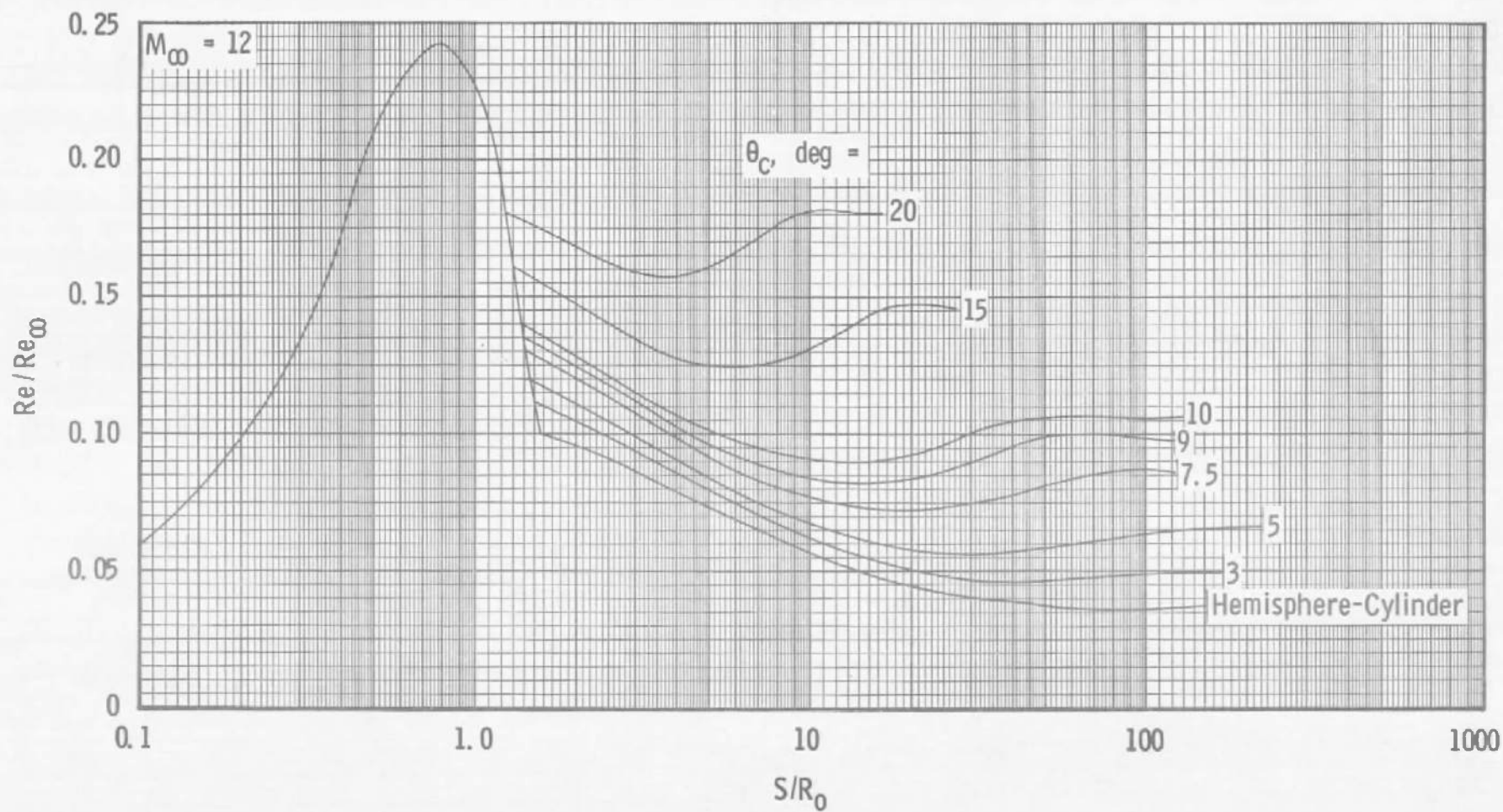


Fig. 5 Continued

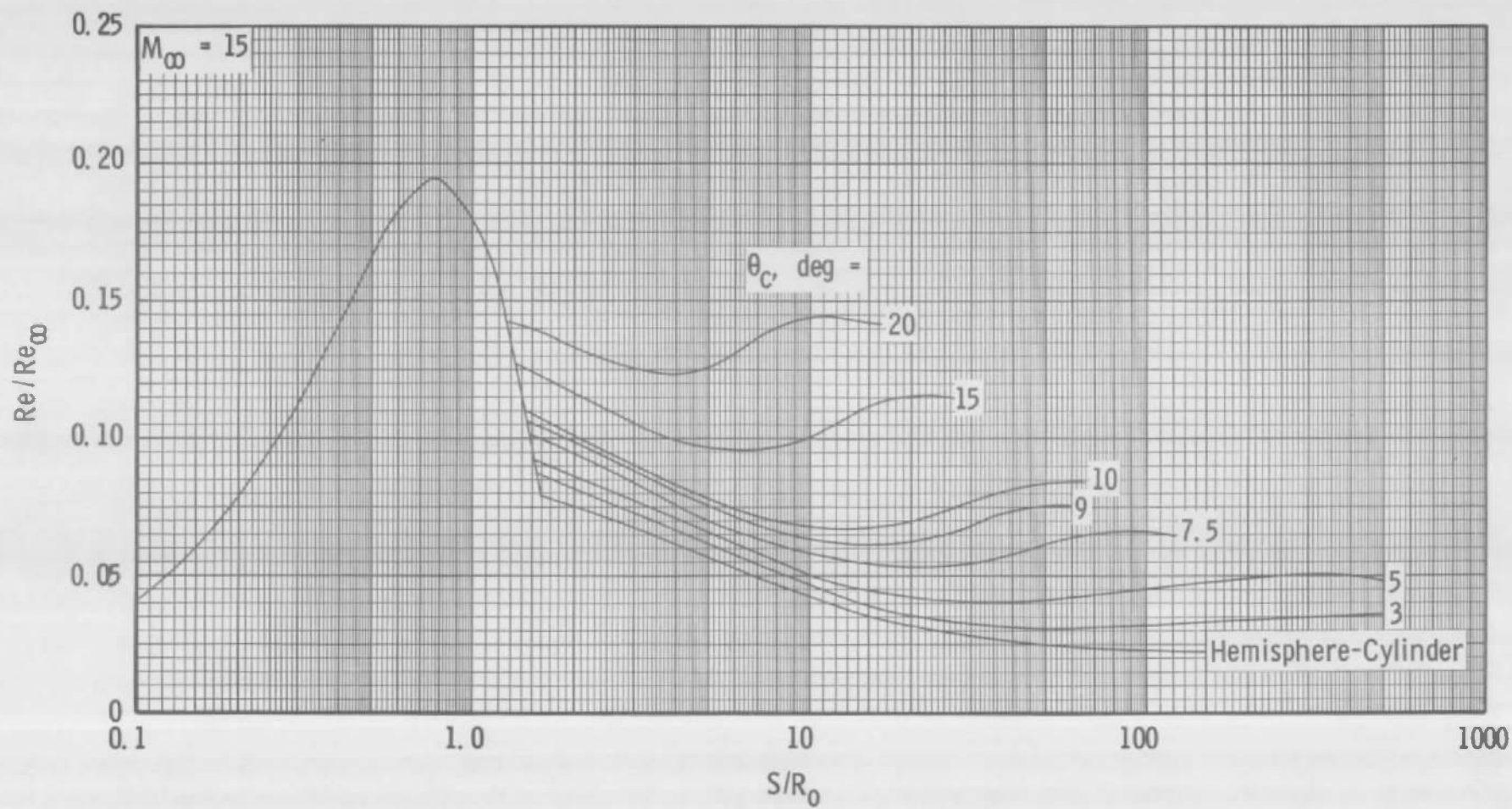


Fig. 5 Continued

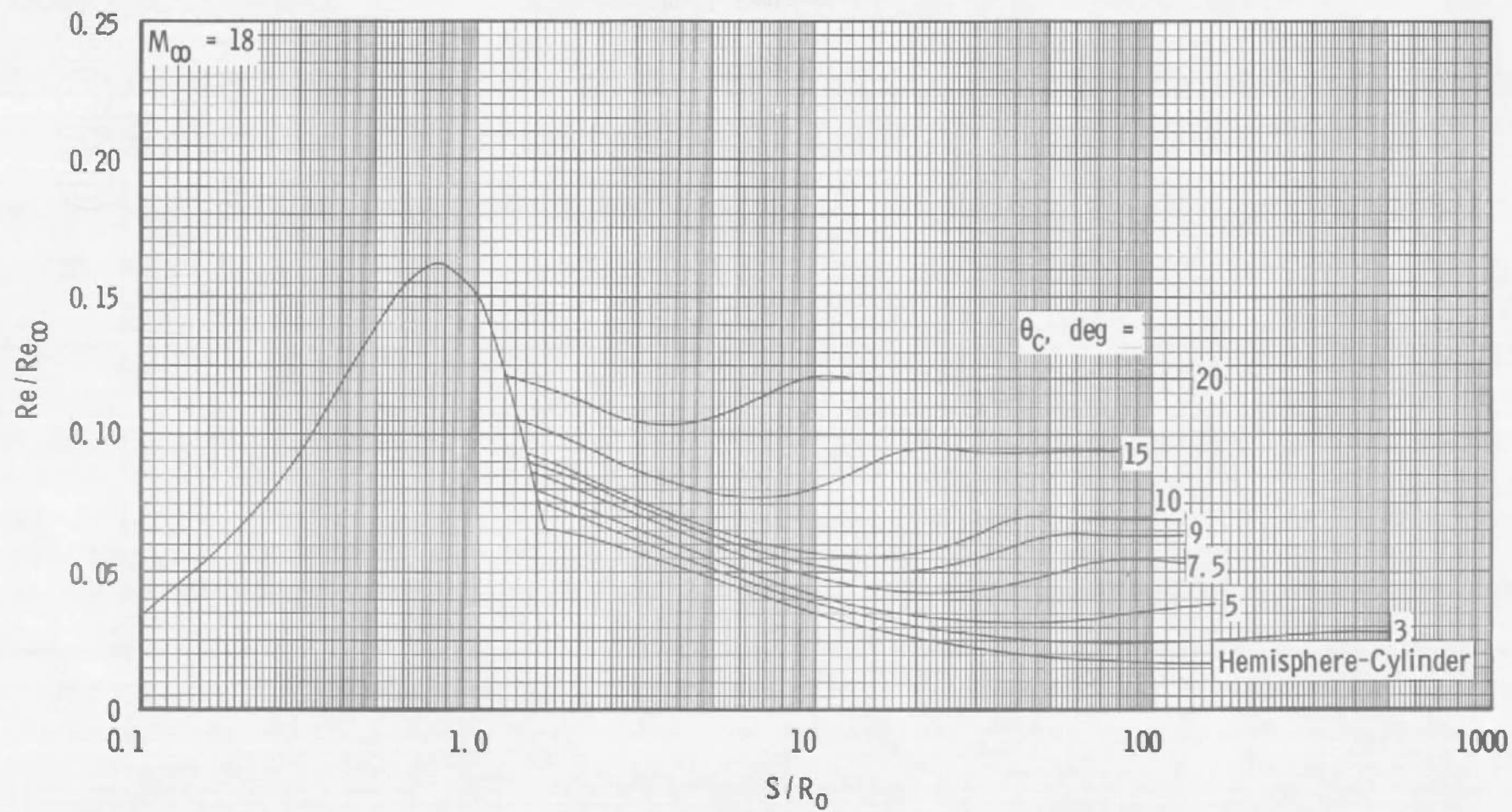


Fig. 5 Continued

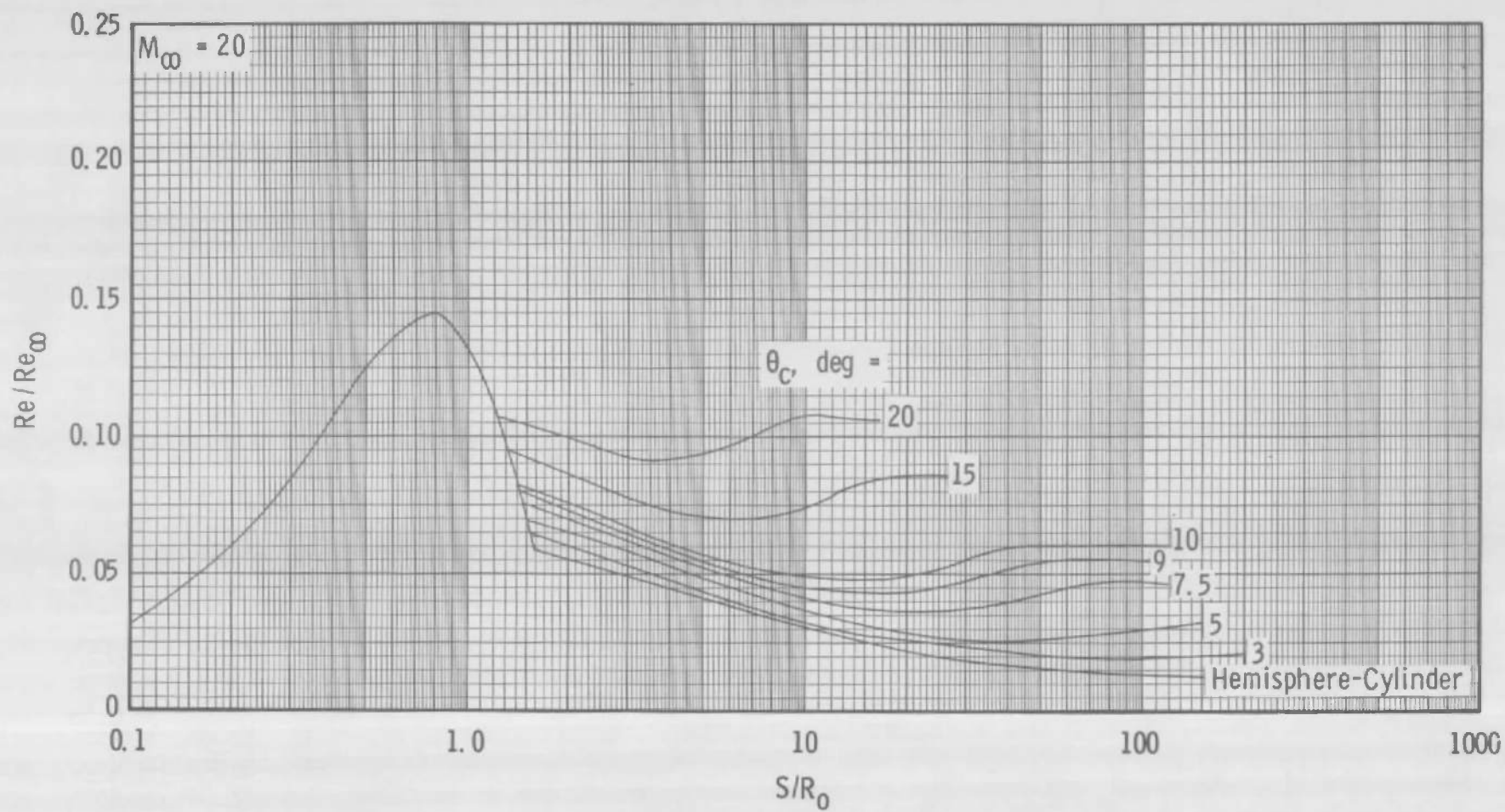


Fig. 5 Continued

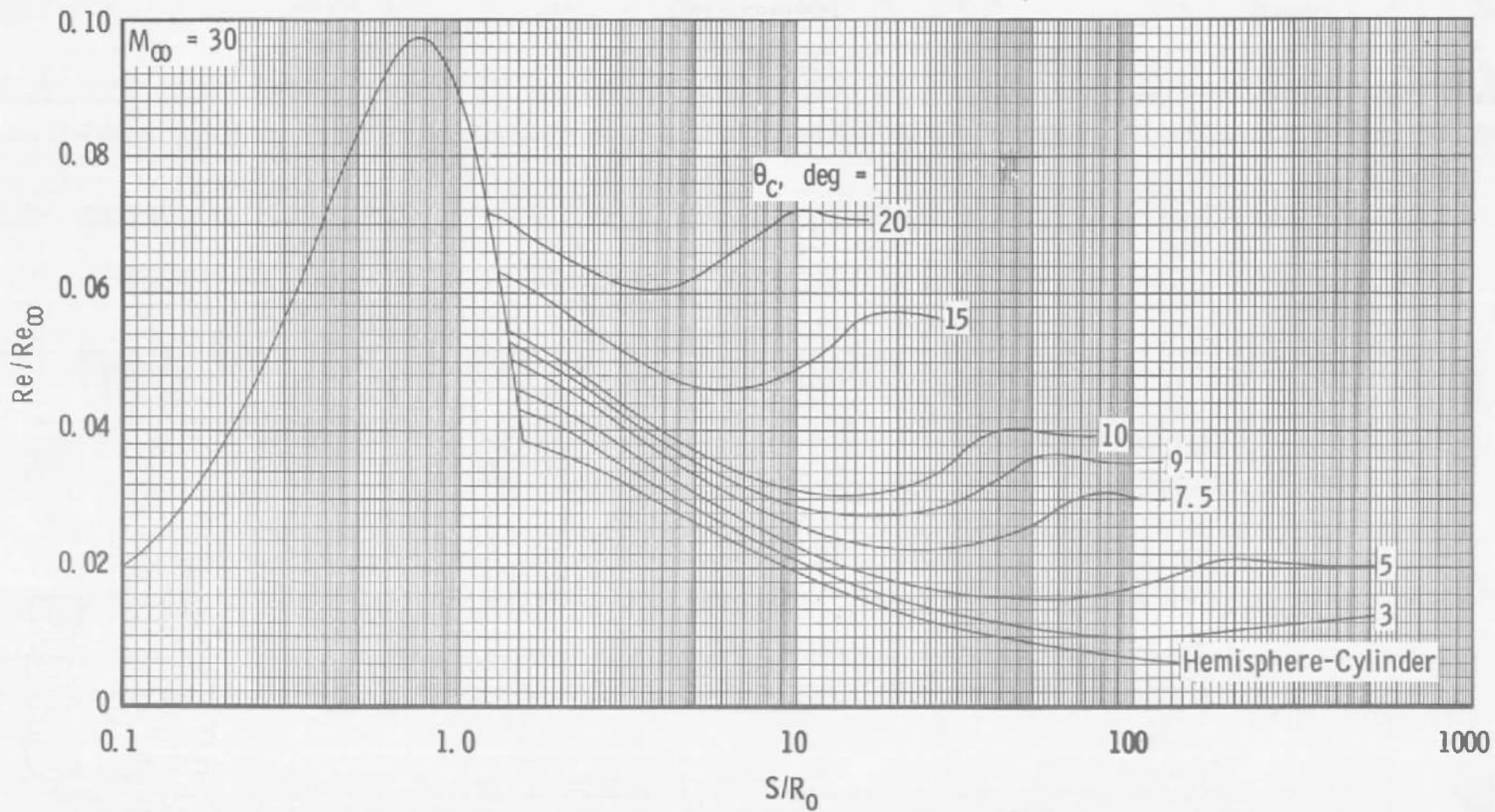


Fig. 5 Concluded

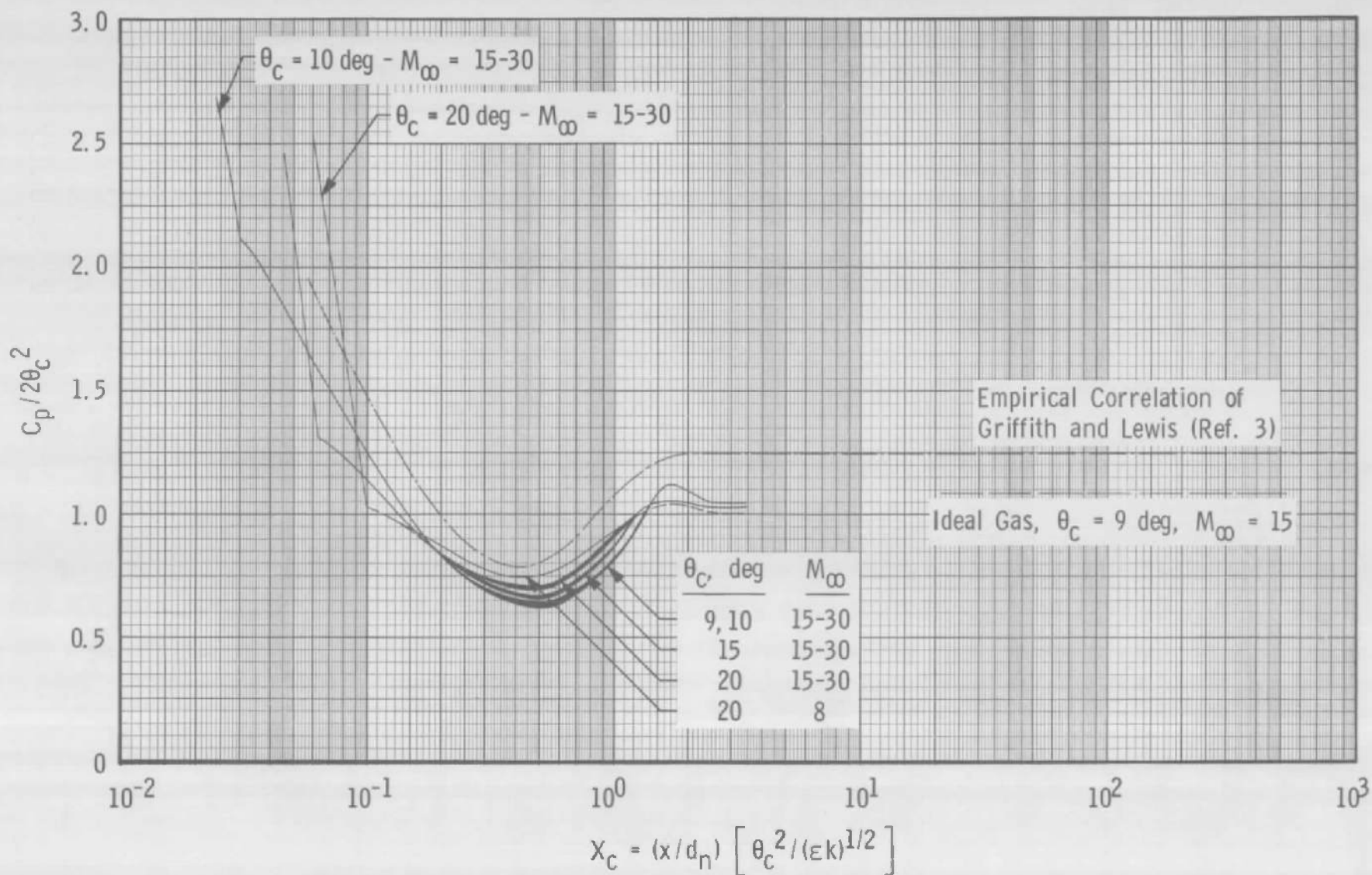


Fig. 6 Correlation of Surface Pressure Distributions for Blunt Cones

DOCUMENT CONTROL DATA - R&D		
(Security classification of title, body of abstract and indexing annotation must be entered when the overall report is classified)		
1 ORIGINATING ACTIVITY (Corporate author) Arnold Engineering Development Center ARO, Inc., Operating Contractor Arnold Air Force Station, Tennessee		2a REPORT SECURITY CLASSIFICATION UNCLASSIFIED
		2b GROUP N/A
3 REPORT TITLE IDEAL GAS SPHERICALLY BLUNTED CONE FLOW FIELD SOLUTIONS AT HYPERSONIC CONDITIONS		
4 DESCRIPTIVE NOTES (Type of report and inclusive dates) N/A		
5 AUTHOR(S) (Last name, first name, initial) Roberts, J. F., Lewis, C. H., and Reed, Marvin, ARO, Inc.		
6 REPORT DATE August 1966	7a TOTAL NO OF PAGES 46	7b NO OF REFS 8
8a CONTRACT OR GRANT NO AF40(600)-1200 b PROJECT NO. 8953 c Program Element 62405334 d Task 895303	9a ORIGINATOR'S REPORT NUMBER(S) AEDC-TR-66-121 9b. OTHER REPORT NO(S) (Any other numbers that may be assigned this report) N/A	
10 AVAILABILITY/LIMITATION NOTICES Qualified users may obtain copies of this document from DDC. Distribution of this document is unlimited.		
11 SUPPLEMENTARY NOTES N/A	12. SPONSORING MILITARY ACTIVITY Arnold Engineering Development Center, Air Force Systems Command, Arnold Air Force Station, Tenn.	
13 ABSTRACT Charts of surface pressures, Mach number, and Reynolds number distributions over spherically blunted cones in an ideal gas ($\gamma = 1.4$) are presented in the ranges $M_\infty = 8$ to 30 and cone half-angles $\theta_c = 0$ to 20 deg. The pressure data are correlated with $C_p/2\theta_c^2$ against $X_c = (x/d_n)[\theta_c^2/(\epsilon k)]^{1/2}$ and compared with a previous empirical correlation of experimental data. The difference in numerical results and empirical correlation of surface pressures is attributed to the viscous-induced pressure increment in the experimental data.		

LINK A

LINK B

LINK C

ROLE

WT

ROLE

WT

ROLE

WT